



1 **Small-molecule inhibitors of the PDZ domain of Dishevelled**
2 **proteins interrupt Wnt signalling**

3
4 Nestor Kamdem ^{1,2}, Yvette Roske ³, Dmytro Kovalskyy ^{4,6} Maxim O. Platonov ^{4,6}, Oleksii
5 Balinskyi ^{4,6}, Annika Kreuchwig ^{1,2}, Jörn Saupe ^{1,2}, Liang Fang ^{2,3}, Anne Diehl ¹, Peter
6 Schmieder ¹, Gerd Krause ¹, Jörg Rademann ^{1,5}, Udo Heinemann ^{2,3}, Walter Birchmeier ³ and
7 Hartmut Oschkinat ^{1,2}.

8
9 ¹ Leibniz-Forschungsinstitut für Molekulare Pharmakologie, Robert-Rössle-Straße 10, 13125 Berlin, Germany

10 ² Institut für Chemie und Biochemie, Freie Universität Berlin, Takustraße 3, 14195 Berlin, Germany

11 ³ Max-Delbrück-Center for Molecular Medicine, Robert-Rössle-Straße 10, 13125 Berlin, Germany

12 ⁴ Enamine Ltd., Chervonotkatska Street 78, Kyiv 02094, Ukraine

13 ⁵ Institut für Pharmazie, Freie Universität Berlin, Königin-Luise-Straße 2 + 4, 14195 Berlin, Germany

14 ⁶ Taras Shevchenko National University, 62 Volodymyrska, Kyiv 01033, Ukraine

15

16 *Correspondence to:* Hartmut Oschkinat (oschkinat@fmp-berlin.de)

17

18 **Abstract**

19 Dishevelled (Dvl) proteins are important regulators of the Wnt signalling pathway, interacting through
20 their PDZ domains with the Wnt receptor Frizzled. Blocking the Dvl PDZ/Frizzled interaction represents
21 a potential approach for cancer treatment, which stimulated the identification of small molecule
22 inhibitors, among them the anti-inflammatory drug Sulindac and Ky-02327. Aiming to develop tighter
23 binding compounds without side effects, we investigated structure-activity relationships of
24 sulfonamides. X-ray crystallography showed high complementarity of anthranilic acid derivatives in the
25 GLGF loop cavity and space for ligand growth towards the PDZ surface. Our best binding compound
26 inhibits Wnt signalling in a dose-dependent manner as demonstrated by TOP-GFP assays ($IC_{50} \sim 50 \mu M$),
27 and Western blotting of β -catenin levels. Real-time PCR showed reduction in the expression of Wnt-
28 specific genes. Our compound interacted with Dvl-1 PDZ ($K_d = 2.4 \mu M$) stronger than Ky-02327 and
29 may be developed into a lead compound interfering with the Wnt pathway.

30

31

32 **KEYWORDS:** Drug Design, NMR, PDZ, Frizzled, Wnt signalling

33



34 INTRODUCTION

35

36 Post synaptic density protein (PSD95), Drosophila disc large tumour suppressor (Dlg1), and Zonula
37 occludens-1 protein (ZO-1) domains termed PDZ appear in 440 copies spread over more than 260
38 proteins of the human proteome (Ponting 1997). They maintain relatively specific protein-protein
39 interactions and are involved, for example, in signalling pathways, membrane trafficking and in the
40 formation of cell-cell junctions (Zhang 2003, Fanning 1996, Kurakin 2007). Hence, they are potentially
41 attractive drug targets (Rimbault 2019, Christensen 2020). PDZ domains consist of about 90 amino acids
42 which fold into two α -helices and six β -strands exposing a distinct peptide-binding groove (Doyle 1996),
43 Lee 2017). The conserved carboxylate-binding loop (GLGF loop) is essential for the formation of a
44 hydrogen bonding network between the PDZ domain and PDZ-binding, C-terminal peptide motifs, in
45 most cases coordinating the C-terminal carboxylate group of the interaction partner. In the respective
46 complexes, the C-terminal residue of the ligand is referred to as P₀; subsequent residues towards the N-
47 terminus are termed P₋₁, P₋₂, and P₋₃ etc. Previous studies have revealed that P₀ and P₋₂ are most critical
48 for PDZ-ligand recognition (Songyang 1997, Schultz 1998).

49 PDZ domains are divided into at least three main classes on the basis of their amino acid preferences at
50 these two sites: class I PDZ domains recognize the motif S/T-X- Φ -COOH (Φ is a hydrophobic residue
51 and X any amino acid). Class II PDZ domains recognize the motif Φ -X- Φ -COOH, whereas class III
52 PDZ domains recognize the motif X-X-COOH. However, some PDZ domains do not fall into any of
53 these specific classes (Pawson 2007, Sheng 2001, Zhang 2003). The Dvl PDZ domains, for example,
54 recognize the internal sequence (KTXXXW) within the frizzled peptide 525(GKTLQSWRRFYH)536
55 (K_D ~ 10 μ M) (Wong 2003, Chandanamali 2009).

56 Dishevelled proteins are modular proteins comprising 500 to 600 amino acids and containing three
57 conserved domains: an N-terminal DIX (**D**ishevelled/**A**xin) domain, a central PDZ domain, and a C-
58 terminal DEP (**D**ishevelled, **E**gl-10 and **P**leckstrin) domain (Wong 2000, Wallingford 2005). They
59 transduce Wnt signals from the membrane receptor Frizzled to downstream components *via* the
60 interaction between Dvl PDZ and Frizzled (Wong 2003), thus it has been proposed as drug target (Klaus
61 2008, Holland 2013, Polakis 2012). Several studies identified internal peptides of the type (KTXXXW)



62 as well as C-terminal peptides of the type ($\Omega\Phi\text{GWF}$) in which Ω is any aromatic amino acid (F, W or
63 Y) as Dvl PDZ targets (Lee 2009, Zhang 2009). Three Dvl homologues, Dvl-1, Dvl-2 and Dvl-3, have
64 been identified in humans and are highly conserved. The sequence identity is 88% between Dvl-3 PDZ
65 and Dvl-1 PDZ and 96% between Dvl-3 PDZ and Dvl-2 PDZ (Supporting Information Figure S1). Dvl
66 proteins are found to be upregulated in breast, colon, prostate, mesothelium, and lung cancers
67 (Weeraratna 2002, Uematsu 2003, Uematsu 2003, Bui 1997, Mizutani 2005). There are several
68 examples of small-molecule inhibitors of Dvl PDZ. NSC668036 (Shan 2005, Wang 2015) is a peptide-
69 mimic compound which interferes with Wnt signalling at the Dvl level. Based on a computational
70 pharmacophore model of NCS668036, additional compounds were later reported (Shan 2012). Known
71 as first non-peptide inhibitor, the 1H-indole-5-carboxylic acid derivative FJ9 (Fujii 2007) showed
72 therapeutic potential. Further examples including Sulindac (Lee 2009), 2-((3-(2-
73 Phenylacetyl)amino)benzoyl)amino)benzoic acid (3289-8625, also called CalBioChem(CBC)-322338)
74 (Grandy 2009, Hori 2018), N-benzoyl-2-amino-benzoic acid analogs (Hori 2018), phenoxyacetic acid
75 analogs (Choi 2016), and Ethyl 5-hydroxy-1-(2-oxo-2-((2-(piperidin-1-yl)ethyl)amino)ethyl)-1H-
76 indole-2-carboxylate (KY-02327) (Kim 2016) have been reported, with the latter showing the highest
77 *in-vitro* affinity (8.3 μM) of all. Despite the existence of the abovementioned inhibitors of Dvl PDZ, the
78 development of tighter-binding, non-peptidic small-compound modulators of the respective functions,
79 binding with nanomolar affinity, is necessary and remains challenging. Here, nuclear magnetic
80 resonance (NMR) spectroscopy was used to detect primary hits and for follow-up secondary screening.
81 The ability of NMR to detect weak intermolecular interactions ($\mu\text{M} < K_D < \text{mM}$) make it an ideal
82 screening tool for identifying and characterizing weakly binding fragments, to be optimized
83 subsequently by chemical modification in order to improve binding (Zartler 2006, Shuker 1996, Zartler
84 2003). Besides NMR, the determination of X-ray crystal structures of selected complexes was
85 fundamental for further design of new compound structures with improved binding. In the first round of
86 screening, a library constructed after computational docking of candidates into the peptide binding site
87 of the Dvl PDZ domains were investigated, followed by secondary screening utilizing a library of 120
88 compounds containing rhodanine or pyrrolidine-2,5-dione moieties.

89 **RESULTS AND DISCUSSION**



90 **PDZ targeted library design**

91 The PDZ targeted library was designed to cover all PDZ domains with available structure. For this, all
92 X-ray and NMR derived PDZ structures were retrieved from the PDB, clustered, and 6 selected centroids
93 were subjected to the virtual screening routine. The clustering of the PDZ domains was performed
94 according to the shapes of their binding sites, rather than backbone conformation. This approach
95 accounts for the importance of surface complementarity of protein-small molecule interactions and the
96 critical contribution of van der Waals interactions to the binding free energy. On another hand, PDZ
97 domains have evolved to recognize a carboxyl group that is mostly derived from the C-terminus of
98 natively binding proteins. Finally, the fact that PDZ can recognize internal motifs (Hillier 1999),
99 including KTXXXW of Frizzled-7 recognised by Dvl PDZ (Wong 2003, Chandanamali 2009), raises
100 the question of what are key binding contributions with PDZ domains: negative charge, hydrogen
101 bonding or shape complementarity (Harris 2003). For this reason, tangible compounds were preselected
102 to have extensive hydrophobic contacts as well as chemical groups that mimic the carboxylic group.
103 Virtual screening was performed with QXP, and the generated complexes were sequentially filtered with
104 a self-designed MultiFilter algorithm. From the resulting 1119 compounds a randomly selected set of
105 250 compounds was subjected to NMR validation.

106

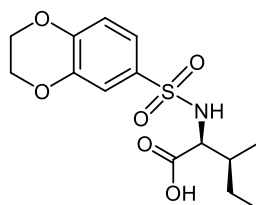
107 **NMR Screening and development of compounds**

108 The results of virtual screening were checked experimentally by comparing 2D ^1H - ^{15}N HSQC
109 (Heteronuclear Single Quantum Correlation) spectra of Dvl-3 PDZ in the absence and presence of the
110 compound to elucidate ligand-induced changes of chemical shifts. Chemical shift perturbation
111 differences (ΔCSPs) were evaluated for compounds that cause shifts of at least three N-H cross-peaks.
112 The responses were classified into: (i) inactive compounds ($\Delta\text{CSP} < 0.02$); (ii) very weak interactions
113 ($0.02 \leq \Delta\text{CSP} \leq 0.05$); (iii) weak interactions ($0.05 < \Delta\text{CSP} \leq 0.1$); (iv) intermediate interactions ($0.1 <$
114 $\Delta\text{CSP} \leq 0.2$); (v): strong interactions ($0.2 < \Delta\text{CSP} \leq 0.5$) and (vi) very strong interactions ($\Delta\text{CSP} > 0.5$).
115 In most cases, the signals of residues S263, V287 and R320 were perturbed (Supporting Information
116 Figure S2). With the ΔCSP of 0.12 ppm, the isoleucine-derived compound **1** ((2,3-
117 dihydrobenzo[b][1,4]dioxin-6-yl)sulfonyl)-L-isoleucine containing a sulfonamide moiety was detected



118 initially as one of the best “hits” according to chemical shift changes. The sulfonamide is a well-known
119 moiety in drug discovery (Mathvink 1999, Wu 1999, Sleight 1998 O’Brien 2000, Tellew 2003).

120

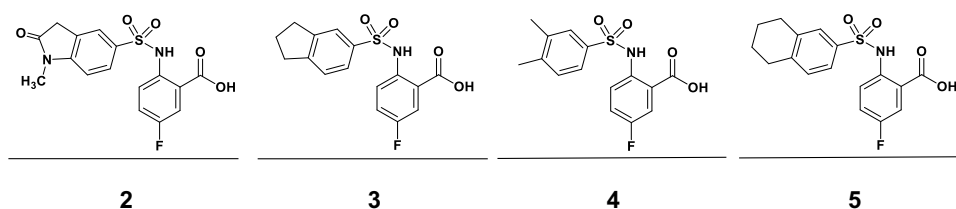


121
122

1

124 Upon NMR titration experiments for compound **1** (Supporting Information Figure S2) with Dvl-3 PDZ,
125 the largest chemical shift perturbations were observed for S263 in strand β B and R320 in helix α B of
126 Dvl-3 PDZ, confirming the conserved binding site.

127



2

3

4

5

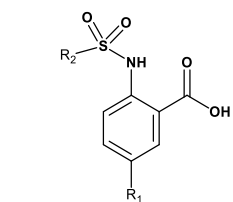
128 **Scheme 1:** Compounds **2, 3, 4, 5**

129 By comparing the binding of several sulfonamide compounds in a secondary screening event and mak-
130 ing use of our in-house library, four new compounds (**2, 3, 4, 5**) that induced chemical shift perturbations
131 larger than 0.2 ppm were found (for binding constants see Table 1) and considered further as reasonably
132 strong binders. The similarity of the structures led us to define Scheme 2 as a scaffold for further refine-
133 ments. Sulfonamides were considered more drug-like, and hence followed up at higher priority than
134 other hits. We realised that our four new compounds had different moieties at R_2 in combination with a
135 small R_1 (fluorine). A decrease of binding was observed with decreasing size of R_2 .

136



137



138 **Scheme 2:** Basic fragment for further synthesis

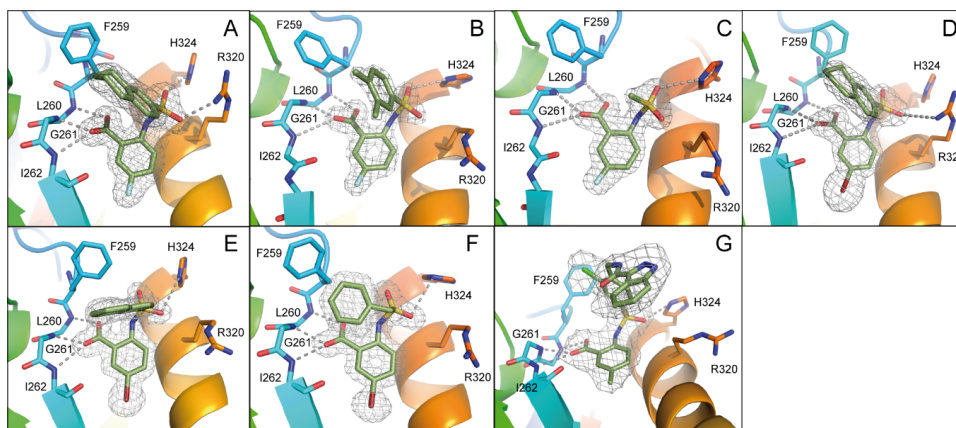
139 In order to assess the importance of the aryl group at R_2 for complex formation, it was replaced by a
140 methyl group as substituent to yield compound **6**, which showed a drastic decrease of binding (Table 1).
141 Compounds **3**, **4**, and **5** did not distinguish between the Dvl-3 PDZ and Dvl-1 PDZ. In order to obtain
142 detailed insight into the binding mode of these compounds, crystal structures of Dvl-3 PDZ in complex
143 with compounds **3**, **5** and **6** were determined (Figure 1). For compound **3** the crystal structure revealed
144 two complexes within the crystallographic asymmetric unit (AU) at 1.43 Å resolution. Both show the
145 anthranilic acid with the attached fluorine pointing into the hydrophobic binding pocket (Figure 1A and
146 Supporting Information Figure S3A), while the carboxyl group forms a hydrogen-bond network with
147 amide residues of the carboxylate binding loop, in particular strand β B (Figure 1A) and specifically with
148 residues I262, G261 and L260. The two sulfonamide oxygen atoms form hydrogen bonds with R320
149 and H324 (weak) of helix α B for only one complex in the AU. The aromatic aryl group
150 (tetrahydronaphthalene) attached to the sulfonamide is involved in hydrophobic interactions with F259
151 (Supporting Information Figure S3B). The 1.6-Å complex structure with compound **5** (4 molecules per
152 AU) exhibits a comparable binding mode as found for compound **3** with a hydrogen-bond network
153 involving the carboxyl group and the amides of I262, G261, L260, and of the sulfonamide to H324
154 (Figure 1B). No hydrogen bond was observed to R320 in all four molecules of the AU, but small
155 variations of the aryl moiety relative to F259 (Supporting Information Figure S3C). The crystals of the
156 complex with **6** show two molecules in the AU (Figure 1C). The sulfonamide is bound by H324 in both
157 complexes (Supporting Information Figure S3D). However, compound **6** bound only in the mM range
158 as compared to **3** and **5**, which obviously results from the missing aromatic rings.
159



	ID	R ₁	R ₂	(K _D , μM) Dvl-3PDZ	(K _D , μM) Dvl-1 PDZ
	2	F		nd	237.6 ± 38.5 ^{NMR}
	3	F		80.6 ± 6.1 ^{NMR}	112.7 ± 25.9 ^{NMR}
	4	F		83.9 ± 7.8 ^{NMR}	114.4 ± 9.8 ^{NMR}
	5	F		140.6 ± 14.1 ^{NMR}	160.1 ± 14.6 ^{NMR}
	6	F	CH ₃	> 1000 ^{ITC}	-
	7	Br		20.6 ± 2.4 ^{NMR}	18.2 ± 2.4 ^{NMR}
	8	CF ₃		17.4 ± 0.5 ^{ITC}	24.5 ± 1.5 ^{ITC}
	9	Cl		41.1 ± 3.1 ^{NMR}	45.6 ± 4.5 ^{NMR}
	10	CH ₃		62.5 ± 4.7 ^{NMR}	60.5 ± 5.3 ^{NMR}
	11	Br		13.8 ^{ITC}	119.9 ^{ITC}
	12	Br		58.5 ^{ITC}	nd
	13	Br		7.2 ^{ITC}	213.2 ^{ITC}
	14	Br		58.1 ± 2.1 ^{ITC}	nd
	15	CF ₃		52.9 ± 1.7 ^{ITC}	nd
	16	CF ₃		59.1 ± 1.5 ^{ITC}	nd
	17	CF ₃		49.5 ^{ITC}	nd
	18	CH ₃		9.4 ± 0.6 ^{ITC}	2.4 ± 0.2 ^{ITC}
	19	CH ₃		21.8 ± 1.7 ^{ITC}	8.0 ± 0.5 ^{ITC}
	20	CH ₃		9.8 ± 0.3 ^{ITC}	4.7 ± 0.3 ^{ITC}
	21	CH ₃		12.5 ± 0.5 ^{ITC}	4.7 ± 0.2 ^{ITC}

160
 161
 162
 163
 164

Table 1. Binding constants K_D (μM) of Dvl-3 PDZ and Dvl-1 PDZ for compounds 3 – 21 derived by ITC or NMR if not specified.



165

166

167 **Figure 1:** Magnified view into crystal structures of various compounds bound to the Dvl-3 PDZ domain. The 2Fo-Fc electron density
168 around the compounds is shown at 1 σ contour level, and the dotted lines indicate formed hydrogen bonds. In the bound
169 compounds covalent bonds to carbon atoms are shown as green sticks. Important residues involved in compound binding are
170 labelled and displayed in atom colours (carbons blue or dark yellow). A-C show compound 3, 5 and 6 respectively. All
171 compounds in A-C contain fluorine (light blue) in para position to the amine. D-F represents the bound compounds 7, 11 and
172 12, respectively. All have bromine (dark red) in para position to the amine. The accession codes of the structures are 6ZBQ,
173 6ZC3, 6ZC4, 6ZC6, and 6ZC8.

174

175

176 To further explore the importance of the fluorine site inside the hydrophobic pocket, substitutions by

177 bromine, chlorine, methyl and trifluoromethyl were chosen. In fact, the methyl group has a similar vdW

178 radius as the CF₃ group. Iodine was not considered a good candidate since it increases molecular weight

179 substantially and the compounds may be chemically less stable, in particular in biological assays. Taking

180 into account that compound 6 did not bind because of the missing aromatic ring at the R₂ position, our

181 strategy was to increase the aromatic ring at R₂ while keeping R₁ as small as possible (preferably CH₃)

182 to enable further compound modifications that fulfil key properties as defined by Lipinski (Lipinski

183 2000, Lipinski 1997). Our preference to continue exploration only at the R₁ position of the aromatic ring

184 in Scheme 1 was inspired by the absence of hits with other substitutions in the secondary screening event

185 and the initial X-ray structures that showed a hydrophobic pocket available for substituents in this

186 position while other sites at the aromatic ring would include steric hindrance. Therefore, compounds 7-

187 17 were obtained and were classified in three different groups to derive structure activity relationships

188 (SAR). The compounds 7-10 in group 1 contain different R₁ (Br, CF₃, Cl, CH₃) but the same moiety

189 (tetrahydronaphthalene) at R₂. As expected, binding could be further improved by displacement of the

190 fluorine with elements exhibiting larger van der Waals (vdW) radii. Indeed, the K_D decreased stepwise

191 and the best fit was observed for compound 8 containing a trifluoromethyl group (K_D = 17.4 μ M for



192 Dvl-3 PDZ and 24.5 μM for Dvl-1 PDZ). The different substituents at the R_2 position contribute to an
193 increased binding affinity in the following order: $\text{F} < \text{Cl} < \text{Br} < \text{CF}_3$ (compound **3** < **9** < **7** < **8**,
194 respectively). Compound **10** with a methyl group at the R_2 position showed only marginally improved
195 binding, although the methyl group has a similar vdW radius as the CF_3 group of compound **8**. The
196 difference in binding results most likely from their different hydrophobicity.

197 The 1.85-Å crystal structure of the Dvl-3 PDZ domain with compound **7** ($K_D = 20.6 \mu\text{M}$ for Dvl-3 PDZ
198 and 18.2 μM for Dvl-1 PDZ) showed an identical hydrogen-bond network involving the amide groups
199 of residues I262, G261 and L260 of the carboxyl binding loop as seen for all other complex structures
200 reported here (Figure 1D). Only one hydrogen bond between the sulfonamide and R320 was found in
201 addition for one of the two Dvl-3 PDZ molecules per AU. H324 of Dvl-3 PDZ was not addressed by the
202 sulfonamide as seen previously. The bromine at position R_1 points into the hydrophobic pocket, similar
203 as the fluorine in the complex structure with compound **3**. The two complexes in the AU show significant
204 variations in the positions of the tetrahydronaphthalene rings as well as for the side chain of F259 and
205 R320 (Supporting Information Figure S3E).

206 Following the analysis of the complex involving compound **7**, the binding characteristics of the group-
207 2 compounds (**11-14**) were investigated. They contain bromine as R_1 and different substituents at the R_2
208 position to assess the importance of π - π stacking interactions involving F259. K_D values of 7.2 μM for
209 compound **13** and 13.8 μM for compound **11** were found with respect to the interaction with Dvl-3 PDZ.

210 Crystal structures of Dvl-3 PDZ in complex with compound **11** (1.58 Å resolution, 1 molecule per AU)
211 and **12** (1.48 Å, 2 molecules per AU) revealed very similar binding as observed in the crystal structures
212 with compounds **3** and **7**. The aromatic rings at R_2 show hydrophobic interactions to F259, but not a
213 classical π - π stacking as expected. Nevertheless, the tighter binding of compound **11** could be explained
214 by the larger aromatic substituent at the R_2 position compared to compound **12**. Both complex structures
215 show also non-specifically bound ligands in crystal contacts (Supporting Information Figure S3H,
216 Supporting Information Tables S2 and S3). The additional ligand molecules in both complex structures
217 can be explained as a crystallographic artefact, which is verified with ITC experiments that indicate 1:1
218 stoichiometries in both cases (Figure S5). With respect to the selectivity of the tested compounds we
219 observed a 6 to 30-fold stronger binding of compounds **7**, **9**, **11** and **13** to Dvl-3 PDZ as compared to



220 Dvl-1 PDZ. These differences are related to the different sequences at the end of α B. Most importantly,
221 H324 is replaced by a serine residue in the Dvl-1 PDZ domain.
222 The group-3 compounds (**15-17**) contain a trifluoromethyl at position R_1 and were tested to investigate
223 a cooperative role of this moiety with various substituents at position R_2 . All compounds bind weaker
224 to Dvl-1 and Dvl-3 than compound **8** which contains tetrahydronaphthalene at the R_1 position, revealing
225 its important role in the interaction.

226

227 **Further modifications towards higher affinity and reduced toxicity**

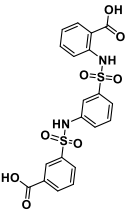
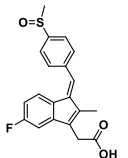
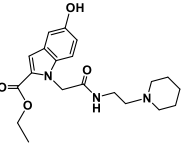
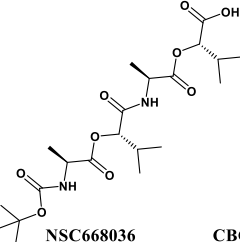
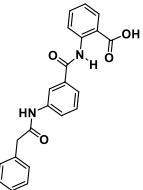
228 Possible cytotoxic effects of compounds **3, 7, 8, 9, and 10** were evaluated in cell viability assays using
229 HEK293 cells (Supporting Information Figure S4). These compounds were selected due to different
230 substituents at the R_1 , including halogens. Cell viability was measured 24h after treatment with the
231 individual compounds, and half maximal inhibitory concentrations (EC_{50}) were calculated for each
232 compound. The compounds exhibited EC_{50} values in the range of 61-131 μ M (Supporting Information
233 Figure S4A). Compounds **3** and **10** that contained fluorine or methyl group substituents at R_2 ,
234 respectively, were the least toxic, while compound **7**, containing bromine, was the most toxic. The
235 results from crystallography, modelling studies and of the cell proliferation assays led us to further
236 investigate compounds **18-21** that contain a methyl group at the R_1 position and different substituents
237 as R_2 . In this way, we aimed to develop both potent and less toxic, cell permeable inhibitors. All
238 compounds showed strong interactions as indicated by chemical shift perturbation values between 0.30
239 to 0.34 ppm (Supporting Information Table S1). The binding constants were evaluated by ITC whereby
240 compound **18** ($K_D = 9.4 \mu$ M for Dvl-3 PDZ and 2.4μ M for Dvl-1 PDZ) appeared to be most potent.
241 Compound **18** contains a pyrazole ring which is considered as an important biologically active
242 heterocyclic moiety (Lv 2010). Compounds **20** ($K_D = 9.8 \mu$ M for Dvl-3 PDZ and 4.7μ M for Dvl-1 PDZ)
243 and **21** ($K_D = 12.5 \mu$ M for Dvl-3 PDZ and 4.7μ M for Dvl-1 PDZ) contain pyrrole rings. Their binding
244 constants almost have the same value despite the different substituents (bromine or chlorine) at the
245 pyrrole rings. The binding of compounds **18-21** to both Dvl PDZ domains is mainly enthalpy-driven as
246 indicated in Table 2, with a slightly stronger effect for Dvl-1 PDZ than for Dvl-3 PDZ. To our surprise,
247 the crystal structure of Dvl-3 PDZ in complex with compound **18** shows the pyrazole substituent in the



248 R₂ position orientated away from the binding pocket. Instead, a π-π stacking interaction with F259 was
 249 observed (Supporting Information Figure S3I). Cytotoxicity of **18-21** was determined *via* MTT assays
 250 (Mosmann 1983) that displayed viability up to concentrations above 150 μM (Supporting Information
 251 Figure S4B).

252

Compound	Dvl-3 PDZ				Dvl-1 PDZ			
	Kd (μM)	ΔH (kcal/ mol)	TΔS (kcal/ mol)	ΔG (kcal/ mol)	Kd (μM)	ΔH (kcal/ mol)	TΔS (kcal/ mol)	ΔG (kcal/ mol)
18	9.4 ± 0.6	-8.0	-1.2	-6.8	2.4 ± 0.2	-12.2	-4.7	-7.5
19	21.0 ± 1.7	-5.9	0.4	-5.5	8.0 ± 0.5	-7.3	-0.3	-7.0
20	9.8 ± 0.3	-10.4	-3.6	-6.8	4.7 ± 0.3	-9.4	-2.2	-7.2
21	12.5 ± 0.5	-5.9	0.7	-6.8	4.7 ± 0.2	-8.5	-1.5	-7.0
NPL-1011	79.7 ± 53.3							
Sulindac	8.3 ± 2.5							
CBC-322338/ 3289-8625	> 400 μM							
NSC668036	> 400 μM							
Ky-02327					8.3 ± 0.8 ^{16g}			

				
NPL-1011	Sulindac	Ky-02327	NSC668036	CBC-322338 / 3289-8625

256

257 **Table 2:** Isothermal titration calorimetric data for the reaction between Dvl-3 PDZ, Dvl-1 PDZ and our compounds **18**, **19**, **20**
 258 and **21** respectively. Compounds NPL-1011 (Hori 2018), and Sulindac (Lee 2009), CBC-322338/3289-8625 (Grandy 2009,
 259 Hori 2018), and NSC668036 (Shan 2005), for more thermodynamic parameters see Supporting Information Figure S7. For Ky-
 260 02327 the value from literature is included.

261

262 Comparison to reported Dvl PDZ-binding molecules

263 Our compounds bind to Dvl-3 with a K_d better than 10 μM, and slightly tighter to Dvl-1, see Table 2,
 264 with **18** showing a K_d of 2.4 μM and chemical shift changes indicating binding to the canonical binding
 265 site (Supporting Information Figure S8). For comparison, four compounds shown in Supporting
 266 Information Figure S6 were assayed by ITC (Supporting Information Figure S7) regarding their affinity
 267 to Dvl-3 PDZ. Ky-02327 was already determined to bind with a K_d of 8.3 ± 0.8 μM (Kim 2016) to Dvl-
 268 1 PDZ. Our first interest was oriented towards sulfonamides. Hori et al (Hori 2018) have recently
 269 reported 3-({3-[(2-carboxyphenyl)sulfamoyl]phenyl}sulfamoyl)benzoic acid (NPL-1011) binding to
 270 Dvl-1 PDZ via the detection of chemical shift changes, and further sulfonamide compounds that showed
 271 smaller effects, indicating weaker binding. We examined the binding constant of NPL-1011 which



272 possesses two sulfonamide moieties by ITC and found a value of $79.7 \pm 53.3 \mu\text{M}$, see Table 2. For
273 further comparisons, we assayed also CBC-322338/3289-8625, Sulindac and NSC668036 by ITC.
274 Surprisingly, CBC-322338/3289-8625 showed very low affinity, with a K_d above $400 \mu\text{M}$ (assumed to
275 be the threshold for our ITC assay), which was larger than the originally reported value (10.6 ± 1.7)
276 (Grandy 2009) and closer to the value found by Hori et al (Hori 2018) ($954 \pm 403 \mu\text{M}$). Concerning
277 non-sulfonamide compounds, a K_d of $8.3 \pm 2.5 \mu\text{M}$ was detected for Sulindac, while NSC668036 (Shan
278 2005) did not show high-affinity binding. These results are largely in agreement with literature. In all
279 cases, compounds were tested for purity after K_d measurements (see Supporting Information Figures
280 S9A-D).

281

282 **Selectivity testing using a set of selected PDZ domains**

283 Compounds **18**, **20** and **21** were tested towards other PDZ domains for selectivity. The set included
284 PSD95-PDZ 2 and 3, Shank-3, α -syn trophin, and AF-6 PDZ. According to the determined chemical
285 shift perturbations (Supporting Information Table S4), our compounds show no or very weak
286 interactions with the selected PDZ domains ($0.05 < \Delta\text{CSP} \leq 0.1$) ppm. These findings led to the
287 conclusion that our compounds show considerable selectivity towards Dvl PDZ domains. This
288 selectivity might be due to a unique feature of Dvl PDZ where R320 (Dvl-3 PDZ) or R322 (Dvl-1 PDZ)
289 are crucial for interactions, explaining selectivity with respect to other PDZ domains. In addition, the
290 large hydrophobic cavity for the side chain of the C-terminal residue of the interacting peptide is
291 occupied by a large moiety in case of compounds **18**, **20** and **21** which might not be accommodated in
292 most other PDZ domains.

293

294 **Dvl inhibitors antagonize canonical Wnt signalling and Wnt-related properties of cancer cells**

295 Taking advantage of a lentivirus that encodes GFP in a β -catenin/TCF-dependent fashion (TOP-GFP,
296 SABiosciences), a stable HEK293 reporter cell line was established to evaluate the inhibitory effect of
297 compounds **18**, **20** and **21** on canonical Wnt signalling activity. TOP-GFP expression in this cell line
298 was induced by the ligand Wnt3a, which directly activates the Frizzled-Dishevelled complex and
299 protects β -catenin from degradation by the destruction complex (Figure 2A). Remarkably, all three
300 compounds inhibited Wnt signalling induced by Wnt3a in a dose-dependent manner (Figure 2B),



301 yielding IC_{50} values between 50-80 μ M. To further evaluate the specificity of our Dvl inhibitors, the
302 conventional TOPflash (Molenaar 1996) and other luciferase reporter assays were performed. In HeLa
303 cells, **20** inhibited TOP-luciferase signals stimulated by Wnt3a but not by CHIR99021 (Sineva 2010), a
304 compound that activates Wnt signalling downstream of Dvl (Figure 2A, C). Compound **20** had no
305 significant inhibitory effects in reporter assays that measure the activity of other signalling systems, e.g.,
306 NF- κ B-luciferase stimulated by recombinant TNF α , Notch-luciferase stimulated by the overexpression
307 of the Notch intracellular domain, or the Oct-luciferase assay that is stimulated by overexpression of
308 Oct4 (SABiosciences, Figure 2D). These results strongly indicate that **20** is specific for canonical Wnt
309 signalling at the upstream level.

310 Increased β -catenin protein level is a hallmark of active Wnt signalling (Kishida 1999). Once β -catenin
311 is accumulated in the cytoplasm, it can translocate into the nucleus and activate the transcription of Wnt
312 target genes by interacting with transcription factors of the TCF/LEF family (Figure 2A) (Behrens
313 1996). In HeLa cells, all three Dvl inhibitors blocked the increase of production of β -catenin by Wnt3a
314 in dose-dependent manners, as seen by Western blotting (Figure 2E). Increased mRNA

315

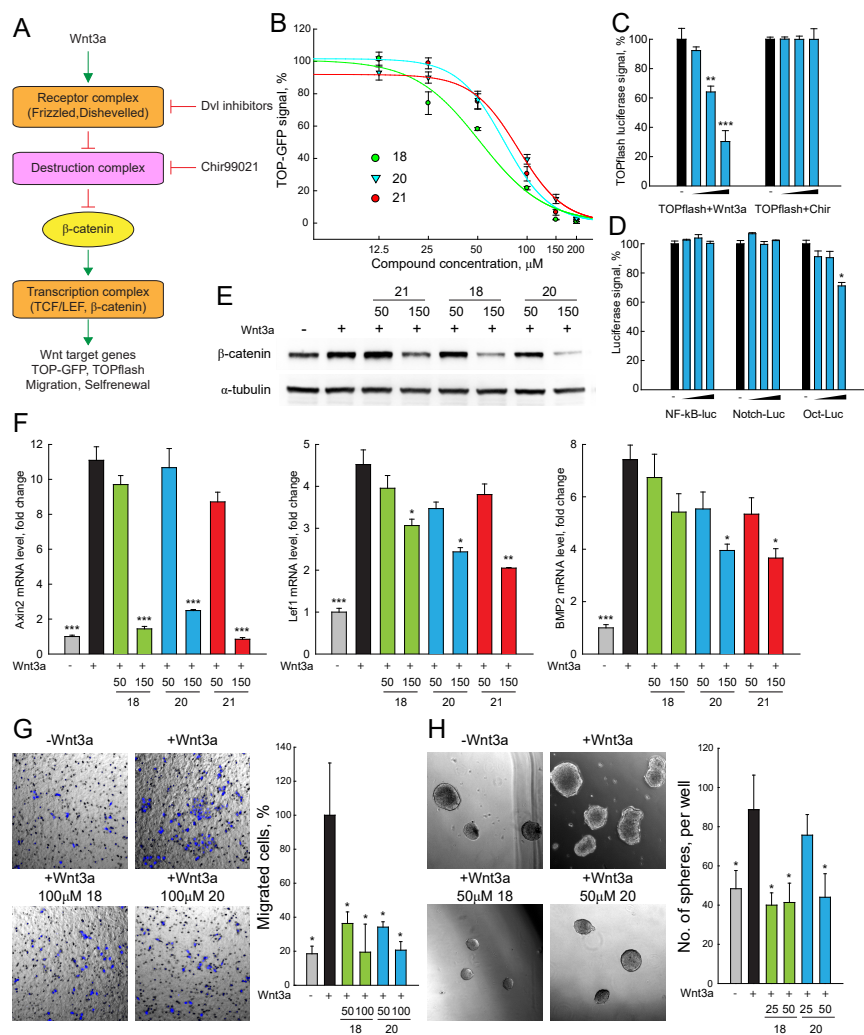


Figure. 2

316
 317
 318
 319
 320
 321
 322
 323

Figure 2. DVL inhibitors antagonize Wnt signalling and Wnt related properties of cancer cells induced by Wnt3a. **A.** Scheme of Wnt signalling pathway. Important components of the Wnt signalling pathway are schematically presented. Wnt3a treatment increases the transcription of Wnt targets, enhances signals of TOP-GFP and TOPflash assays, and promotes Wnt related biological properties of cancer cells. **B.** TOP-GFP reporter assays were performed with HEK293 reporter cell line. Compound **18**, **20** and **21** inhibited Wnt3a induced Wnt activation in dose-dependent manner with IC₅₀ of 50~75 μM. **C&D.** TOPflash assays stimulated with Chir99021 and reporter assays of other pathway were used to evaluate the specificity of compound **20**. Compound **20** specifically inhibited Wnt3a induced Wnt activation, and had no or mild effect on Chir99021 induced Wnt



324 activation and other signalling pathways including NF- κ B, Notch and Oct4. E. β -Catenin protein levels were detected with
325 Western blotting in HeLa cells. Compound **18**, **20** and **21** (150 μ M) inhibited accumulation of β -catenin in HeLa cells treated
326 with Wnt3a. F. The mRNA levels of Wnt target genes (Axin2, Lef1 and Bmp2) in HeLa cells were measured with quantitative
327 real-time PCR. Compounds **18**, **20** and **21** (150 μ M) reduced the transcription of Wnt target genes that are enhanced by Wnt3a
328 treatment in HeLa cells. G. Cell migration of SW480 cells after Wnt3a treatment was assessed by transwell assays. Compounds
329 **18** and **20** (50–100 μ M) reduced the migration of SW480 cells enhanced by Wnt3a. H. SW480 cells were cultured in serum-
330 free non-adherent condition to evaluate the self-renewal property enhanced by Wnt3a treatment. Compound **18** and **20** (25–50
331 μ M) reduced sphere formation of SW480 cells that was enhanced by Wnt3a treatment.
332

333 levels of the Wnt target genes Axin2, Lef1 and Bmp2 (Riese 1997, Jho 2002, Lewis 2010) were induced
334 by Wnt3a treatment, as measured by qRT-PCR, and these increases were reduced by compounds **18**, **20**
335 and **21** (Figure 2F). These results demonstrate that compounds **18**, **20** and **21** inhibit Wnt signalling as
336 indicated by reduced accumulation of β -catenin and low expression of typical Wnt target genes.

337 Canonical Wnt signalling contributes to cancer progression by inducing high motility and invasion of
338 cancer cells while retaining the self-renewal property of cancer initiating cells (Fritzmann 2009, Sack
339 2011, Vermeulen 2010, Malanchi 2008). In particular, cancer initiating cells are propagated and
340 enriched in non-adherent sphere culture, demonstrating the self-renewal capacity of the stem cells
341 (Kanwar 2010, Fan 2011). To investigate the potential value of the Dvl inhibitors for interfering with
342 these Wnt-related properties of cancer cells, the subline SW480WL was derived from the SW480 colon
343 cancer cell line, which exhibits a low level of endogenous Wnt activity (Fang 2012). The cell migration
344 and self-renewal properties of SW480WL cells were enhanced by Wnt3a treatment, as revealed by
345 transwell and sphere formation assays (Figure 2G, H). Compounds **18** and **20** prevented increased cell
346 migration and sphere formation. These results indicate that our Dvl inhibitors may be developed into
347 lead compounds that interfere with Wnt signalling.
348

349 CONCLUSIONS

350 In the present work, small molecules that bind to Dvl PDZ in the one-digit micromolar range with
351 considerable selectivity have been developed by an extensive structure-based design approach. With
352 regards to the affinity determined by ITC, compound **18** binds to Dvl-1 and Dvl-3 in vitro with Kd
353 values of 2.4 and 9.4, respectively, comparing very well with known ligands. X-ray structures of Dvl-3
354 PDZ complexes with selected compounds provided insight into crucial interactions and served as the
355 basis for the design of tight binding compounds with reduced toxicity. The structural investigations
356 revealed that these compounds form hydrogen bonds with the amide groups of residues L260, G261 and



357 I262 in the PDZ-domain loop and the side chains of residues H324 and R320. Finally, the chosen
358 methodology, virtual screening followed by a two-stage NMR based screening, X-ray crystallography,
359 and chemical synthesis is an excellent path towards bioactive interaction partners. Our best compounds
360 effectively inhibited the canonical Wnt signalling pathway in a selective manner and could be developed
361 for further studies.

362

363 **Experimental Section**

364 **Clustering binding sites and selection of representative PDZ domains**

365 Three-dimensional structures of PDZ domains were retrieved from the PDB (Berman 2000). At the time
366 of the study from a total of 266 PDB files, 126 were NMR solution structures and 140 derived from X-
367 ray diffraction studies. The structures belong to 163 PDZ domains of 117 different proteins from 11
368 organisms. Files which contain more than one 3D conformation for a domain (up to 50 for NMR-derived
369 data) were split into separate structures and considered independently. The total number of unique 3D
370 structures was 2,708.

371 Amino acid sequences of PDZ domains were aligned using Clustal Omega software (Sievers 2011).
372 Based on the alignment, for each structure, residues which form the binding site (strand β B and helix
373 α B) were determined (Supporting Information Figure S8). The centre of the binding site was defined as
374 a geometric centre of $C\alpha$ atoms of 7 residues (6 residues from the β B strand and the second residue from
375 the α B helix). Such bias toward the β B strand was made to cover sites occupied by residues in -1 and -
376 3 positions.

377 The triangulated solvent accessible surface for each PDZ structure was built using MSMS software
378 (Sanner 1996) with a spherical probe radius of 1.4 Å and vertex density 10 Å⁻¹. The largest connected
379 set of surface vertices within 9 Å from the centre of the binding site was used to construct shape-based
380 numerical descriptors. The descriptors are 508-dimensional vectors of non-negative integer numbers
381 and were built using a shape distributions approach (Osada 2002). In total 10 (Pawson 2007) vertex
382 triplets were selected randomly, each forming a triangle. Triangles which had a side longer than 16 Å
383 were discarded. Triangle sides were distributed into 16 length bins, each 1 Å wide, covering lengths
384 from 0 to 16 Å. A combination of three sorted side lengths, each belonging to one of 16 distance bins,



385 defines one of 508 categories of the triangles. The number of triangles of each category was calculated,
386 resulting in a 508-dimensional vector which is used as a numerical descriptor of the binding pocket
387 shape. For further operations with descriptors, Euclidian metric was introduced. Shape descriptors were
388 distributed into 6 clusters using k-means algorithm (Jain 1988). For each cluster, a centroid structure
389 was defined as the one, whose descriptor is the closest to mean descriptor for the cluster. The centroid
390 structures (2O2T#B.pdb, 1VA8#3.pdb, 2DLU#01.pdb, 1UHP#8.pdb, 2OS6#8.pdb, 3LNX#A.pdb) were
391 used for docking.

392

393 **PDZ targeted library design**

394 Screening collection by Enamine Ltd. (Chuprina 2010) containing a total of 1,195,395 drug-like
395 compounds was used as the primary source of small molecules. Natural ligand of PDZ is the C-terminus
396 of a peptide with carboxylic group making extensive hydrogen bond network with the “ΦGΦ” motif.
397 Since the carboxyl provides either of negative charge and hydrogen bond acceptor, we want our ligands
398 to retain at least one of these features. Therefore, we pre-filtered the stock library to bear chemical
399 groups which have negatively charged and/or hydrogen bond acceptor functionality. In total 65,288
400 compounds were selected for the virtual screening study. The selected 6 centroids of PDZ domains and
401 the prepared compound set were subjected to high-throughput docking using the QXP/Flo software
402 (McMartin 1997). Complexes were generated with 100 steps of *sdock* + routine, and 10 conformations
403 per complex were saved.

404 Processing of docking poses started with filtering by contact term *Cntc* from the QXP/Flo scoring
405 function. Entries with *Cntc* < 45 were discarded, which removed complexes with weak geometries of
406 bound ligands. The remained filtering was performed with the in-house MultiFilter program that allows
407 flexible geometry-based filtering. We applied two algorithms, *nearest-atom* filter and *hydrogen-bond*
408 filter. The former filters complexes by distance from a given protein atom to the nearest heavy ligand
409 atom, while in the latter, filtering is based upon the number of hydrogen bonds calculated for a given
410 complex geometry. With the *nearest-atom* routine we selected compounds that filled the P₀ pocket and
411 sterically mimicked binding of a peptide carboxylic group. Peptide group hydrogens of the “ΦGΦ” motif
412 and atoms forming the hydrophobic pocket were used for that. With the *hydrogen-bond* filter we selected



413 compounds that formed extensive hydrogen bonding with the PDZ domain. Both these properties might
414 have larger impact on binding rather than negative charge (Harris 2003). Details on atoms used for
415 filtering and thresholds for *hydrogen-bond* filtering, as well as the resulting number of compounds, are
416 provided in Supporting Information Table S5. Compounds from complexes which passed through these
417 filters were incorporated into a targeted library for the PDZ-domain family. The final library contained
418 1119 compounds in total.

419

420 **Screening of compounds**

421 Two-dimensional ^1H - ^{15}N HSQC spectra were used to screen a library of 212 compounds designed by
422 the company Enamine for PDZ domains. 50 μM of ^{15}N -labeled protein samples were prepared in a 20
423 mM sodium phosphate buffer, containing 50 mM sodium chloride, 0.02% (w/v) NaN_3 , at pH 7.4. Stock
424 solutions of small molecules were prepared in *DMSO- d_6* at a concentration of 160 mM. A ^1H - ^{15}N HSQC
425 spectrum of Dvl PDZ was acquired at 300 K with 5% *DMSO- d_6* in the absence of ligand as reference
426 spectrum. Mixtures of 16 compounds were added to ^{15}N -labeled Dvl PDZ at 8-fold molar excess each.
427 The final concentration of *DMSO- d_6* in the protein-ligand solutions was 5%. Spectra were acquired
428 with 8 scans and 256 points in the indirect dimension. Compound binding was deduced if the resonance
429 position of a cross-peak was significantly shifted compared to the reference spectrum. The active
430 compound was obtained through successive deconvolution. Experiments were recorded on a Bruker
431 DRX600 spectrometer equipped with a triple-resonance cryoprobe. The preparation of samples was
432 done automatically by a Tecan Genesis RSP 150 pipetting robot. Spectra were analysed using the
433 programs TOPSPIN and SPARKY.⁴⁷

434

435 **Synthesis of compounds**

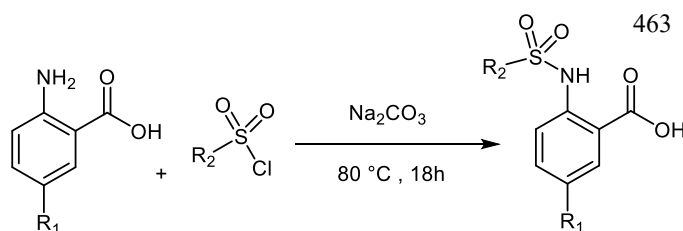
436 All reagents and starting materials were purchased from Sigma-Aldrich Chemie GmbH, ABCR GmbH
437 & Co.KG, alfa Aesar GmbH & Co.KG or Acros Organics and used without further purification. All air
438 or moisture-sensitive reactions were carried out under dry nitrogen using standard Schlenk techniques.
439 Solvents were removed by evaporation on a Heidolph Laborota 4000 with vacuum provided by a PC
440 3001 Vaccubrand pump. Thin-layer chromatography (TLC) was performed on plastic-backed plates pre-



441 coated with silica gel 60 F₂₅₄ (0.2 mm). Visualization was achieved under an ultraviolet (UV) lamp (254
442 and 366 nm). Flash chromatography was performed using J.T Baker silica gel 60 (30-63 μm). Analytical
443 high-performance liquid chromatography (HPLC) was performed on a Shimadzu LC-20 (degasser
444 DGU-20A3, controller CBM-20A, autosampler SIL-20A) with a DAD-UV detector (SPD-M20A),
445 using a reverse-phase C18 column (Nucleodur 100-5, 5 μM, 250 mm x 4 mm, Macherey-Nagel, Düren,
446 Germany). Separation of compounds by preparative HPLC was performed on a Shimadzu LC-8A
447 system equipped with a UV detector (SPD-M20A), using a semi-preparative C18 column (Nucleodur
448 100-5, 5 μM, 250 mm x 10 mm, Macherey-Nagel) or preparative C18 column (Nucleodur 100-5, 5 μM,
449 250 mm x 21 mm, Macherey-Nagel). The detection wavelength was 254 nm. Gradients of acetonitrile-
450 water with 0.1% TFA were used for elution at flow rates of 1 mL/min, 8 mL/min, and 14 mL/min on
451 the analytical, semi-preparative and preparative columns respectively. Melting points (mp) were
452 determined with Stuart Melting Point Apparatus SMP3 and are not corrected. Mass spectra were
453 recorded on a 4000Q TRAP LC/MS/MS/ System for AB Applied Biosystems MDS SCIEX. NMR
454 spectra were recorded on a Bruker AV300 spectrometer instrument operating at 300 MHz for proton
455 frequency using DMSO-*d*₆ solutions. Chemical shifts were quoted relative to the residual DMSO peak
456 (¹H: δ = 2.50 ppm, ¹³C: δ = 39.52 ppm). Coupling constants (J) are given in Hertz (Hz). Splitting patterns
457 are indicated as follows: singlet (s), doublet (d), triplet (t), quartet (q), multiple (m), broad (b). Purity of
458 each compound used for biological testing was ≥95% unless otherwise noted. The purity check of known
459 inhibitors purchased for comparison with our compounds are found in Supporting Information Figure
460 S9.

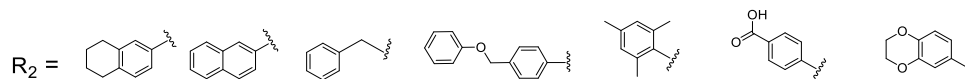
461

462 **Synthesis of compounds 8, 11 – 17**





R₁ = CF₃, Br, Cl



465 **Scheme 3:** Synthesis of compounds 8, 11 - 17

466 To a solution of anthranilic acid substituted with the appropriate R₁ (1.32 mmol) and sodium carbonate
467 (3.17 mmol) in water (2 mL) at 80 °C, the sulfonyl chloride (1.58 mmol) substituted with the appropriate
468 R₂ was added over a period of 5 minutes. The stirring continued for 18 h at 80 °C. The reaction mixture
469 was cooled to room temperature and acidified with 6 N HCl, and the resulting solid precipitate was
470 filtered, washed with water and dried to give the crude product. The final product was obtained by
471 preparative HPLC (Puranik 2008).

472

473 **2-(5,6,7,8-tetrahydronaphthalene-2-sulfonamido)- 5- (trifluoromethyl) benzoic acid (8)**

474 (0.52 g, 74% yield) ¹H-NMR (300 MHz, DMSO-d₆): δ = 11.77 [s, 1H, COOH], 8.13 [s, 1H, NH],
475 7.85 [d, ³J_{6,4} = 2.1 Hz, 1H, 6-H_{Ar}] 7.62 [d, ⁴J_{1',3'} = 2.1Hz, 1H, 1'-H_{Ar}] 7.53 [dd, ³J_{4,3} = 7.1 Hz, ⁴J_{4,6} =
476 2.1 Hz, 4-H_{Ar}] 7.36 [dd, ³J_{3',4'} = 7.5 Hz, ⁴J_{3',1'} = 2.4 Hz, 1H, 3'-H_{Ar}] 7.15 [d, ³J_{4',3'} = 7.5Hz, 1H,4'-H_{Ar}]
477 , 6.90 [d, ³J_{3,4} = 7.1Hz, 1H, 3-H_{Ar}] 2.73 (m, 4H, CH₂); 1.6 (m, 4H, CH₂); ¹³C-NMR (75 MHz, DMSO-
478 d₆): δ = 169.1(C, C_{Ar}-8), 152.7(C, C_{Ar}-2), 143.8 (C, C_{Ar}-4a'), 138.7(C, C_{Ar}-2'), 135.9 (C, C_{Ar}-8a'),
479 130.4(CH, C_{Ar}-4), 128.7 (CH, C_{Ar}-6), 127.5 (CH, C_{Ar}-1'), 124.0 (CH, C_{Ar}-4'), 121.6 (C, C-6), 118.2 (C,
480 C_{Ar}-5), 116.9 (C, C_{Ar}-3), 29.0 (CH₂, C-8'), 28.8 (CH₂, C-5'), 22.3 (CH₂, C-6'), 22.2 (CH₂, C-7'); mp:
481 177°C; MS (ESI) *m/z*:calcd. for C₁₈H₁₆F₃NO₄S, 399; found 400 [M+H]⁺.

482 **5-bromo-2-(naphthalene-2-sulfonamido) benzoic acid (11)**

483 (0.13 g, 67% yield) ¹H-NMR (300 MHz, DMSO-d₆): δ = 10.2 [s, 1H, COOH], 9.8 [s, 1H, NH] 8.59 [d,
484 ⁴J_{1',3'} = 1.4 Hz, 1 H, 1'-H_{Ar}], 8.17 [d, ³J_{8',7'} = 7.8 Hz, 1 H, 8'-H_{Ar}], 8.10 [d, ³J_{4'3'} = 8.8 Hz, 1 H, 4'-H_{Ar}],
485 8.02 [d, ³J_{5',6'} = 7.8 Hz, 1 H, 5'-H_{Ar}], 7.93 [d, ⁴J_{6,4} = 2.4 Hz, 1 H, 6-H_{Ar}], 7.77 [dd, ³J_{3',4'} = 8.8 Hz, ⁴J_{3',1'}
486 = 1.4Hz, 1 H, 3'-H_{Ar}], 7.72 – 7.65 [m, 3 H, 4-H_{Ar}, 6'-H_{Ar}, 7'-H_{Ar}], 7.51 [d, ³J_{3,4} = 8.9 Hz, 1 H, 3-H_{Ar}]. –
487 ¹³C-NMR (75 MHz, DMSO-d₆): δ = 168.2 (C, C-7), 138.8 (C, C_{Ar}-2), 136.8 (CH, C_{Ar}-4), 135.3 (C, C_{Ar}-
488 4a'), 134.4 (C, C_{Ar}-8a'), 133.4 (CH, C_{Ar}-6), 131.4 (CH, C_{Ar}-6'), 129.3 (CH, C_{Ar}-4'), 128.5 (CH, C_{Ar}-



489 8'), 127.8 (2xCH, C_{Ar}-5', C_{Ar}-7') 121.6 (CH, C_{Ar}-3'), 120.6 (CH, C_{Ar}-3), 119.0 (C, C_{Ar}-1), 114.9 (C, C_{Ar}-
490 5). Mp: 199°C; (ESI) *m/z*: calcd. for C₁₇H₁₁BrNO₄S⁻; 403.9560; found 403.9613 [M-H]⁻.

491 **5-bromo-2-(phenylmethanesulfonamido)benzoic acid (12)**

492 (0.07g, 42% yield) ¹H-NMR (300 MHz, DMSO-d₆): δ = 10.57 [s, 1 H, COOH], 8.05 [d, ⁴J_{6,4} = 2.4
493 Hz, 1 H, 6-H_{Ar}], 7.75 [dd, ³J_{4,3} = 8.9 Hz, ⁴J_{4,6} = 2.4 Hz, 1 H, H-4_{Ar}], 7.49 [d, ³J_{3,4} = 8.9 Hz, 1 H, 3-H_{Ar}],
494 7.33 – 7.28 [m, 3 H, 3'-H_{Ar}, 5'-H_{Ar}], 7.23 – 7.20 [m, 2 H, 4'-H_{Ar}], 5.75 [s, 1 H, NH], 4.72 [s, 2 H, 1'-
495 H] ¹³C-NMR (75 MHz, DMSO-d₆): δ = 168.3 (C, C-7), 139.9 (C, C_{Ar}-2), 137 (CH, C_{Ar}-4), 133.4 (CH,
496 C_{Ar}-6), 130.7 (CH, C_{Ar}-3'), 128.6 (C, C_{Ar}-2'), 128.4 (CH, C_{Ar}-5'), 128.3 (CH, C_{Ar}-4'), 119.5 (CH,
497 C_{Ar}-3), 117.5 (C, C_{Ar}-1), 113.9 (C, C_{Ar}-5), 57.4 (CH₂, C-1'). Mp: 216°C; (ESI) *m/z*: calcd. for
498 C₁₄H₁₁BrNO₄S⁻ 367.9860; found 367.9878 [M-H]⁻.

499 **5-bromo-2-(4-(phenoxy)methyl)phenylsulfonamido)benzoic acid (13)**

500 (0.6 g, 29% yield) ¹H-NMR (300 MHz, DMSO-d₆): δ = 7.97 [d, ⁴J_{6,4} = 2.4 Hz, 1 H, 6-H_{Ar}], 7.85 (d,
501 ³J_{2,3'} = 8.3 Hz, 2 H, 3'-H_{Ar}), 7.73 [dd, ³J_{4,3} = 8.9 Hz, ⁴J_{4,6} = 2.4 Hz, 1 H, 4-H_{Ar}], 7.63 [d, ³J_{2,3'} = 8.3 Hz, 2
502 H, 2'-H_{Ar}], 7.47 [d, ³J_{3,4} = 8.9 Hz, 1 H, 3-H_{Ar}], 7.29 [dd, ³J_{3'',2''} = ³J_{3'',4''} = 7.3 Hz, 2 H, 3''-H_{Ar}], 7.00 – 6.92
503 [m, 3 H, 4''-H_{Ar}, 2''-H_{Ar}], 5.17 [s, H, 5'-H]. – ¹³C-NMR (75 MHz, DMSO-d₆): δ = 168.2 (C, C-7),
504 157.9 (C, C_{Ar}-1''), 143.2 (C, C_{Ar}-4'), 138.8 (C, C_{Ar}-2), 137.5 (C, C_{Ar}-1'), 136.9 (CH, C_{Ar}-4) 133.5 (CH,
505 C_{Ar}-6), 129.4 (CH, C_{Ar}-3''), 128.1 (CH, C_{Ar}-2'), 127.0 (CH, C_{Ar}-3'), 120.9 (CH, C_{Ar}-4''), 120.5 (CH, C_{Ar}-
506 3), 119.0 (C, C_{Ar}-1), 114.9 (CH, C_{Ar}-5), 114.7 (CH, C_{Ar}-2''), 68.0 (CH₂, C-5') Mp: 175°C; (ESI) *m/z*:
507 calcd for C₂₀H₁₅BrNO₅S⁻ 459.9860 found 459.9878 [M-H]⁻.

508 **5-bromo-2-(2,4,6-trimethylphenylsulfonamido)benzoic acid (14)**

509 (0.6 g, 78% yield) ¹H-NMR (300 MHz, DMSO-d₆): δ = 11.77 [s, 1H, COOH], 9.98 [s, 1H, NH], 7.68
510 [d, ³J_{6,4} = 7.4 Hz, 1H, 6-H_{Ar}], 7.51 [dd, ³J_{4,3} = 7.1 Hz, ⁴J_{4,6} = 7.4 Hz, 1H 4-H_{Ar}], 7.17 [d, 2H, 4'-H_{Ar}, 6'-
511 H_{Ar}], 7.14 [d, ³J_{3,4} = 1H, 3-H_{Ar}], 2.56 [s, 6H, CH₃, 9'-H, 7'-H], 2.21 [s, 3H, CH₃, 8'-H]; ¹³C-NMR (300
512 MHz, DMSO-d₆): δ = 168.8 (C, C-7), 143.3 (C, C_{Ar}-2), 139.5 (C, C_{Ar}-2'), 139.0 and 139.0 (2x C, C_{Ar}-
513 3', C_{Ar}-1') 137.3 (CH, C_{Ar}-4), 134.0 (CH, C_{Ar}-6'), 133.0 (CH, C_{Ar}-6), 132.5 and 132.5 (2x CH, C_{Ar}-4',
514 C_{Ar}-6') 119.1 (CH, C_{Ar}-3), 117.9 (C, C_{Ar}-5), 114.3 (C, C_{Ar}-1), 22.5 and 22.5 (2 x CH₃, C-7', C-9') 20.7
515 (CH₃, C-8'); mp: 185; MS (ESI): *m/z* 399 [M+H]⁺.
516

517 **2-(4-acetylphenylsulfonamido)-5-(trifluoromethyl)benzoic acid (15)**



518 (0.4 g, 63% yield) **¹H-NMR** (300 MHz, DMSO-d₆): δ = 12.28 [s, 1H, *COOH*]; 12.10 [s, 1H, *NH*], 8.11
519 [d, ⁴J_{6,4} = 2.5 Hz, 1H, 6-H_{Ar}], 8.08 [d, ³J_{3',2'} = 7.5 Hz, 2H, 3'-H_{Ar}], 7.86 [dd, ⁴J_{4,6} = 2.5 Hz, ³J_{4,3} = 7.3 Hz,
520 1H, 4-H_{Ar}], 7.64 [d, ³J_{4,3} = 7.3 Hz, 1H, 3-H_{Ar}], 7.56 [dd ³J_{2',3'} = 7.5 Hz, ⁴J_{2',6'} = 2.3 Hz, 2H, 2'-H_{Ar}, 6'-
521 H_{Ar}] 7.22 [dd, ³J_{3',2'} = 7.5 Hz, ⁴J_{3',5'} = 2.1 Hz, 2H, 3'-H_{Ar}, 5'-H_{Ar}] 2.50 [s, 3H, CH₃, 8'-H]; - **¹³C-NMR**
522 (75 MHz, DMSO-d₆): δ = 197.9 (C, C-7'), 169.1 (C, C-8), 151.8 (C, C_{Ar}-2) 143.5 (C, C_{Ar}-1'), 142.5 (C,
523 C_{Ar}-4'), 140.6 (CH, C_{Ar}-4), 131.4 (CH, C_{Ar}-7), 129.6 (2XCH, C_{Ar}-3', C_{Ar}-5'), 128.6 (2XCH, C_{Ar}-2', C_{Ar}-
524 6'), 127.6 (C, C_{Ar}-6), 123.0 (C, C_{Ar}-5), 118.7 (CH, C_{Ar}-3), 27.3 (CH₃, C-8'); mp: 170°C; MS (ESI) *m/z*
525 : calcd. for C₁₆H₁₂F₃NO₅S. 387; found 388 [M+H]⁺.

526 **2-(2,3-dihydrobenzo[*b*][1,4]dioxine-6-sulfonamido)-5-(trifluoromethyl)benzoic acid (16)**

527 (0.4 g, 65% yield) **¹H-NMR** (300 MHz, DMSO-d₆): δ = 11.48 [s, 1H, *COOH*], 8.13[s, 1H, *NH*], 7.89
528 [d, ⁴J_{6,4} = 3.9 Hz, 1H, 6-H_{Ar}] 7.66 [dd, ³J_{4,3} = 7.2 Hz, ⁴J_{4,6} = 4.3 Hz, 1H, 4-H_{Ar}],
529 7.23 [d, ³J_{4,3} = 7.2 Hz 1H, 3-H_{Ar}], 7.11 [dd, ³J_{2',3'} = 7.3 Hz, ⁴J_{2',8'} = 3.2 Hz, 1H, 2'-H_{Ar}] 6.95 [d, ⁴J_{2',8'} =
530 3.2 Hz, 1H, 8'-H_{Ar}] 4.23 – 4.31 [m, 4H, 5'-H, 6'-H]; - **¹³C-NMR** (75-MHz, DMSO-d₆): δ = 168.9(C,
531 C-8), 148.3 (C, C-4'), 143.8 (C, C-2), 143.5 (C, C-7'), 131.3 (C, C-1'), 130.8 (CH, C-4), 128.6(CH, C-
532 6), 125.7 (C, C-7), 122.1 (C, C-5), 120.9(CH, C-2'), 118.3 (CH, C-3), 118.1(CH, C-3'), 116.8 (CH, C-
533 8'), 64.7(CH₂, C-5') 64.3 (CH₂, C-6'); mp: 178°C; MS (ESI) *m/z*: calcd. for C₁₆H₁₂F₃NO₆S. 403; found
534 404 [M+H]⁺.

535 **5-(trifluoromethyl)-2-(2,4,6-trimethylphenylsulfonamido)benzoic acid (17)**

536 (0.38 g, 62% yield) **¹H-NMR** (300 MHz, DMSO-d₆): δ = 12.28 [s, 1H, *COOH*], 11.60 [s, 1H, *NH*], 8.15
537 [d, ⁴J_{6,4} = 4.3 Hz, 1H, 6-H_{Ar}] 7.92 [dd, ³J_{4,3} = 7.9 Hz, ⁴J_{4,6} = 2.1 Hz, 1H, 4-H_{Ar}] 7.87 [d, ⁴J_{6',4'} = 1.9 Hz, 2H,
538 4'-H_{Ar}, 6'-H_{Ar}], 7.48 [d, ³J_{3,4} = 7.9 Hz, 1H, 3-H_{Ar}], 2.60 [s, 6H, CH₃, 9'-H, 7'-H], 2.23 [s, 3H, CH₃,
539 8'-H]; - **¹³C-NMR** (75 MHz, DMSO-d₆): δ = 169.3 (C, C-7), 154.2 (C, C-2), 143.6 (C, C-2'), 139.1
540 and 139.1 (2xC, C-1', C-3') 132.9 (C, C-5'), 132.5 (CH, C-4), 131.5 and 131.5 (2xCH, C-4', C-6'),
541 130.1(CH, C-6), 128.7 (C, C-8), 122.5 (C, C-5), 117.0 (CH, C-3), 109.0 (C, C-1) ,22.4 and 22.4
542 (2xCH₃, C-7', C-9'), 20.8 (CH₃, C-8'); mp: 184°C; MS (ESI) *m/z*: calcd. for C₁₇H₁₆F₃NO₄S; 387; found
543 388 [M+H]⁺.

544



545 **18, 19, 20, and 21** were purchased from Enamine, Kiev, Ukraine as pure compounds (see also Table S6,
546 Supporting Information).

547

548 **Determination of ligand binding and binding constant by NMR**

549 50 μM of ^{15}N -labeled protein samples were prepared in a 20 mM sodium phosphate buffer containing
550 50 mM sodium chloride, 0.02 % (w/v) NaN_3 , at pH 7.4. Stock solutions of small molecules were
551 prepared in $\text{DMSO-}d_6$ at a concentration of 160 mM. A ^1H - ^{15}N HSQC spectrum of Dvl PDZ was
552 acquired at 300 K with 5% $\text{DMSO-}d_6$ in the absence of ligand as reference spectrum. Mixtures of 16
553 compounds were added to ^{15}N -labeled Dvl PDZ at 8-fold molar excess each. The final concentration of
554 $\text{DMSO-}d_6$ in the protein-ligand solutions was 5%. Spectra were acquired with 8 scans and 256 points
555 in the indirect dimension.

556 Binding was deduced if the resonance position of a cross-peak was significantly shifted compared to the
557 reference spectrum. The active compound was obtained through successive deconvolution. Experiments
558 were recorded on a Bruker DRX600 spectrometer equipped with a triple-resonance cryoprobe. The
559 preparation of samples was done automatically by a Tecan Genesis RSP 150 pipetting robot. Spectra
560 were analysed using the programs TOPSPIN and SPARKY.

561 Chemical shift perturbations were obtained by comparing the ^1H - ^{15}N backbone resonances of protein
562 alone to those of protein-ligand complex. The mean shift difference ($\Delta\delta$ in ppm) was calculated using
563 the equation 1 (Garrett 1997, Bertini 2011).

564

$$565 \quad \Delta\delta = \sqrt{\left[\frac{1}{2}(\Delta\delta_H)^2 + \frac{1}{25}(\Delta\delta_N)^2\right]} \quad (\text{Eq. 1})$$

566 Here $\Delta\delta_N$ and $\Delta\delta_H$ are the amide nitrogen and amide proton chemical shift differences between the free
567 and the bound states of the protein. In order to estimate binding constants, titration experiments
568 monitored by NMR were done. A series of ^1H - ^{15}N HSQC were recorded as a function of ligand
569 concentration. Residues showing a continuous chemical shift change and for which the intensity
570 remained strong were classified as being in fast exchange. The dissociation binding constant was
571 estimated by fitting the observed chemical shift change to equation 2 (Shuker 1996, Hajduk 1997).



$$\begin{aligned} 572 \quad & \frac{\Delta\delta}{\Delta\delta_{max}} \\ 573 \quad & = \frac{([L_T] + [P_T] + K_D) - \sqrt{([L_T] + [P_T] + K_D)^2 - 4[L_T] \cdot [P_T]}}{2[P_T]} \quad (Eq. 2) \end{aligned}$$

574

575 $\Delta\delta$ is the observed protein amide chemical shift change at a given compound concentration and $\Delta\delta_{max}$
576 the maximum chemical shift change at saturation. $[L_T]$ the total concentration of the compound, and $[P_T]$
577 the total concentration of the protein. K_D is the equilibrium dissociation constant. The K_D values are
578 reported as means \pm standard deviations of at least six residues influenced upon binding of the ligand.

579

580 **Determination of binding constant by Isothermal Titration Calorimetry (ITC)**

581 Isothermal Titration Calorimetry (ITC) experiments were performed using a VP-ITC system
582 (MicroCal). Protein in 20 mM Hepes buffer, 50 mM NaCl, pH 7.4, was centrifuged and degassed before
583 the experiment. A 200 μ M ligand solution containing 2% DMSO was injected 30 times in 10 μ L aliquots
584 at 120 s intervals with a stirring speed of 1000 rpm into a 1.4 mL sample cell containing the Dvl PDZ
585 domain at a concentration of 20 μ M at 25 °C. Control experiment was initially determined by titrating
586 ligand into buffer at same conditions. Titration of ligand into buffer yielded negligible heats.
587 Thermodynamic properties and binding constants were determined by fitting the data with a nonlinear
588 least-squares routine using a single-site binding model with Origin for ITC v.7.2 (Microcal).

589

590 **Protein expression**

591 PDZ domains of human AF6 (P55196-2, residues 985–1086) and murine α 1-syntrophin (Q61234,
592 residues 81–164) were cloned into pGEX-6P-2 (Amersham Biosciences, Freiburg, Germany) and
593 pGAT2 (European Molecular Biology Laboratory, Heidelberg, Germany), respectively. Proteins were
594 expressed in *E. coli* BL21 (DE3) cells and purified as previously described (Boisguerin 2004). For the
595 cloning of the Dvl-1 PDZ domain (O14640, residues 245–338), IMAGp958J151157Q (ImaGenes) was
596 used as template. V250 is exchanged to isoleucine as in human Dvl-3 or murine Dvl-1. The C-terminal
597 C338 of the domain was exchanged by serine. Via cloning in pET46EK/LIC, a coding sequence for a
598 TEV (Tobacco Etch Virus) protease cleavage site was introduced. The resulting plasmid pDVL1 was



599 transformed in *E. coli* BL21 (DE3). Expression on two-fold M9 minimal medium with 0.5 g/L ¹⁵N
600 NH₄Cl as sole nitrogen source in shaking culture was done at 25 °C overnight with 1 mM IPTG. A yield
601 of 25 mg of pure Dvl-1 was obtained from 1 L culture after IMAC, TEV protease cleavage, a second
602 IMAC, and gel filtration (Superdex 75). The protein domain Dvl-1_{245–338} was supplied for NMR in
603 20 mM phosphate buffer, pH 7.4, 50 mM NaCl.

604 The production of Dvl-3 (Q92997 residues 243-336), mShank3 (Q4ACU6, residues 637-744) PDZ
605 domains and the 3 PDZ domains of PSD95 was described by Saupe et al (Saupe 2011).

606

607 **Crystallization and X-ray diffraction**

608 The His-tagged cleaved human Dvl-3 PDZ domain was concentrated to 12-20 mg/mL in the presence
609 of a 5-fold molar excess of compound **3**, **5**, **6**, **7**, **11** and **12**. Crystals of all complexes were grown at
610 room temperature by the sitting drop vapour-diffusion method. 200 nL Dvl-3/compound solution was
611 mixed with an equal volume of reservoir solution using the Gryphon (Formulatrix) pipetting robot.
612 Crystals of all complexes were grown to their final size within 4 to 14 days. The Dvl-3 PDZ domain
613 crystallized in complex with compound **3** and **7** in crystallization condition 30% PEG 8000, 0.2 M
614 ammonium sulphate, 0.1 M MES pH 6.5; with compound **5** in 30% PEG 8000, 0.1 M MES pH 5.5; with
615 compound **6** in 1.2 M ammonium sulphate, 0.1 M citric acid pH 5.0; with compound **12** in 32% PEG
616 8000, 0.2 M ammonium sulphate, 0.1 M Na-cacodylate pH 6.0; with compound **11** in 1 M ammonium
617 sulphate, 1% PEG 3350, 0.1 M Bis-Tris pH 5.5; with compound **12** in 1.26 M sodium phosphate, 0.14
618 M potassium phosphate and with compound **18** in 1.5 M ammonium sulphate, 12% glycerol, 0.1 M Tris-
619 HCl pH 8.5. The crystals were cryoprotected if necessary, for data collection by soaking for few seconds
620 in precipitant solution containing 20% (v/v) glycerol and subsequently frozen in liquid nitrogen.
621 Diffraction data were collected at 100 K at beamline BL14.1 at the synchrotron-radiation source BESSY,
622 Helmholtz-Zentrum Berlin and processed with XDS.

623

624 **Structure determination and refinement**

625 Phases for the Dvl-3 PDZ domain in complex with compound **3** were obtained by molecular replacement
626 with PHASER (McCoy 2007) using the *Xenopus laevis* Dishevelled PDZ domain structure (PDB code



627 2F0A) as a starting model. The reasonable crystal packing and electron density allowed further model
628 and compound building using the program COOT (Emsley 2004) with iterative refinement with
629 REFMAC (Murshudov 1997). All further complex structures were obtained in the same way but using
630 the final refined compound free Dvl-3-PDZ structure as model for molecular replacement. The
631 Ramachandran statistics were analysed by Molprobit (Chen 2010) for all complexes and all
632 crystallographic statistics are given in Supporting Information Tables S2 and S3. Figures were prepared
633 with PyMol. Atomic coordinates and structure factor amplitudes for DVL-3 PDZ domain in complex
634 with compound **3**, **5**, **6**, **7**, **11**, **12**, **18** were deposited in the Protein Data Bank with accession codes
635 6ZBQ, 6ZBZ, 6ZC3, 6ZC4, 6ZC6, 6ZC7 and 6ZC8, respectively.

636

637 **MTT assay**

638 HEK293 cells were plated on a 96-well plate and treated with different concentrations of Dvl inhibitors.
639 After 24 h treatment, 20 μ l of MTT solution (5 mg/mL) was added into each well. After 2 h incubation,
640 cell culture medium was replaced with 50 μ L DMSO, and the signal of the purple formazan, produced
641 by living cells, was measured by a plate reader.

642

643 **TOP-GFP reporter assay**

644 The lentivirus particle (CCS-018L, SABiosciences) encoding GFP under the control of a basal promoter
645 element (TATA box) joined to tandem repeats of a consensus TCF/LEF binding site was transfected
646 into HEK293 cells. Stable cells were selected by puromycin (2 μ g/mL) treatment. Wnt signalling
647 activity indicated by GFP intensity was measured by flow cytometry after 24 h incubation with
648 recombinant mouse Wnt3a (100 ng/mL) or GSK3 inhibitor CHIR99021 (3 μ M) in the presence of Dvl
649 inhibitors.

650

651 **Luciferase reporter assays**

652 Plasmids encoding a firefly luciferase reporter gene under the control of different responsive elements
653 were transfected into Hela cells with a pRL-SV40 normalization reporter plasmid using the
654 Lipofectamine 2000 (Invitrogen). After desired treatment, cells were harvested in the passive lysis buffer



655 (Promega), and 15 μ L cell lysate were transferred to 96-well LumiNunc plates (Thermo Scientific).
656 Firefly luciferase and Renilla luciferase were detected with the D-luciferin buffer (75 mM Hepes, 4 mM
657 $MgSO_4$, 20 mM DTT, 100 μ M EDTA, 0.5 mM ATP, 135 μ M Coenzyme A and 100 μ M D-Luciferin
658 sodium salt, pH 8.0) and the coelenterazine buffer (15 mM Na_4PPi , 7.5 mM NaAc, 10 mM CDTA, 400
659 mM Na_2SO_4 , 25 μ M APMBT and 1.1 μ M coelenterazine, pH 5.0) respectively using the CentroXS
660 LB960 lumimeter (Berthold Technologies).

661

662 **Immunoblotting**

663 To assess the β -catenin accumulation in HeLa cells, cells were treated with Wnt3a in the presence of Dvl
664 inhibitors for 24 h and lysed in RIPA buffer (50 mM Tris, pH 8.0, 1% NP-40, 0.5% deoxycholate, 0.1%
665 SDS, 150 mM NaCl). Equal amounts of protein were loaded on a SDS-PAGE. Separated proteins were
666 blotted onto PVDF membranes for immunoblot analysis using anti- β -catenin antibody (610154, BD).
667 HRP-conjugated anti-mouse antibody (715-035-150, Jackson ImmunoResearch laboratories) was used
668 for secondary detection with Western lightning chemiluminescence reagent plus (PerkinElmer) and
669 Vilber Lourmat imaging system SL-3.

670

671 **qRT-PCR analysis**

672 To measure the Wnt target accumulation at mRNA level, HeLa cells were treated with Wnt3a in the
673 presence of Dvl inhibitors for 24 h. mRNA was extracted according to the standard TRIzol® protocol
674 (Invitrogen) and reverse-transcribed using random primers (Invitrogen) and M-MLV reverse
675 transcriptase (Promega). The qRT-PCR was performed in iQ5 Multicolor Real-Time PCR Detection
676 System (Bio-Rad) using SYBR® Green (Thermo Scientific) and gene-specific primer pairs of Bmp2,
677 Axin2, Lef1 and β -actin (endogenous control).

678

679 **Migration assay**

680 Cell motility was assessed using 24-well transwell (pore diameter: 8 μ m, Corning). SW480WL cells
681 were seeded in the upper chamber in serum free DMEM with 0.1% BSA; 20% serum was supplemented
682 to medium in the lower chamber. After incubation with Wnt3a in the presence of Dvl inhibitors for 24



683 h, nonmigrant cells were scraped off using a cotton swab; the migrated cells on the filters were stained
684 with DAPI, photographed and counted.

685

686 **Colon sphere culture**

687 SW480WL cells were trypsinised into single cells, seeded on 24-well cell culture plates precoated with
688 250 µl polyhema (12 mg/mL in 95% ethanol, Sigma) per well, and incubated with Wnt3a in the presence
689 of Dvl inhibitors in the sphere culture medium (F12 : DMEM 1 : 1, 1X B-27 supplement, 20 ng/mL
690 EGF, 20 ng/mL FGF, 0.5% methylcellulose) for 10 days. Numbers of spheres were then counted under
691 the microscope.

692

693 **Notes**

694 The authors declare no competing financial interest.

695

696 **ACKNOWLEDGEMENTS**

697 This research was supported by the Deutsche Forschungsgemeinschaft (DFG) Research Group 806 and
698 the EU-project iNext (Infrastructure for NMR, EM and X-rays for Translational Research, GA 653706).
699 We thank M. Leidert and S. Radetzki for protein preparation, and B. Schlegel for NMR assistance. We
700 also thank E. Specker for compound analysis.

701 **ABBREVIATIONS USED**

702 NMR, nuclear magnetic resonance; HSQC, Heteronuclear Single Quantum Correlation;
703 AU, asymmetric unit; SAR, derive structure activity relationships; vdW, van der Waals;
704 ITC, Isothermal titration calorimetry; PDZ, PSD95/Disc large/Zonula occludens 1);
705 Dvl, Dishevelled; PPI, protein-protein interactions; PDB, Protein Data Bank;
706 CSP, chemical shift perturbation; GFP, green fluorescent protein; DMSO, dimethyl sulfoxide;
707 PEG, polyethylene glycol; RNA, ribonucleic acid; mRNA, messenger RNA;
708 qRT-PCR, quantitative real-time polymerase chain reaction; DMEM Dulbecco's modified Eagle's
709 medium ; BSA, bovine serum albumin;

710



711 **ASSOCIATED CONTENT**

712

713 **Accession Codes**

714 Atomic coordinates and structure factor amplitudes for DVL3 PDZ domain in complex with compound
715 **3, 5, 6, 7, 11, 12, 18** were deposited in the Protein Data Bank with accession codes 6ZBQ, 6ZBZ, 6ZC3,
716 6ZC4, 6ZC6, 6ZC7 and 6ZC8, respectively. Authors will release the atomic coordinates and
717 experimental data upon article publication.

718

719 **Supporting information**

720 **1.** Structure-based alignment of the amino acid sequences of Dvl-1,2,3 PDZ ; PSD95-PDZ-1,2,3 ; Af-
721 6 and Syn PDZ domains. (S.2)

722 **2.** 1H-15N HSQC spectra of Dvl-3 PDZ domain alone and in the presence of varying concentrations of
723 compound 3. (S.3)

724 **3.** Detailed views of diverse compounds bound to the Dvl-3 PDZ domain. (S.4)

725 **4.** Cell viability assays of compounds 3, 7,8, 9, 10, (A) and 18, 20, 21 (B). (S.5)

726 **5.** ITC binding assays of compound 18 with Dvl-3 PDZ (A) and with Dvl-1 PDZ (B). (S.5)

727 **6.** Structures of selected compounds used for comparison to our compounds. (S.6)

728 **7.** ITC data of selected compounds used for comparison to our compounds. (S.7)

729 **8.** Definition of PDZ binding site. (S.8)

730 **9.** Purity check of compounds. (S.9)

731 – Purity check of NPL-1011 compound. (S.9)

732 – Purity check of Sulindac compound. (S.10)

733 – Purity check of CalBioChem-322338 compound. (S.11)

734 – Purity check of NSC668036 compound. (S.12)

735 – LCMS of intermediate compound 8. (S.13)

736 – LCMS of intermediate compound 14. (S.13)

737 **10.** Chemical shift perturbation values of Dvl-3 PDZ and Dvl-1 PDZ for compounds (3-21). (S.14)

738 **11.** Data collection and refinement statistics of compounds 3, 5, 6, 7. (S.15)



- 739 **12.** Data collection and refinement statistics of compounds 11, 12, 18. (S.16)
- 740 **13.** Selectivity of ligands derived from chemical shift perturbation of compounds tested at other PDZ
741 domains. (S.17)
- 742 **14.** Details of Multifilter routines. (S.17)
- 743 **15.** Smiles codes and Compounds ID. (S.18)
- 744 **16.** NMR characterization of synthesized compounds (8, 11, 13, 14, 15, 16, 17). (S.21)
745
- 746 **References**
- 747 Behrens, J., von Kries, J. P., Kühl, M., Bruhn, L., Wedlich, D., Grosschedl, R. and Birchmeier, W.:
748 Functional interaction of beta-catenin with the transcription factor LEF-1. *Nature*, 382, 638-642,
749 DOI: 10.1038/382638a0, 1996.
- 750 Bertini, I., Chevanace, S., Del Conte, R., Lalli, D. and Turano, P.: The anti-apoptotic Bcl-x(L) protein,
751 a new piece in the puzzle of cytochrome c interactome. *PLoS One*, 6:e18329, DOI:
752 10.1371/journal.pone.0018329, 2001.
- 753 Berman, H. M., Westbrook, J., Feng, Z., Gilliland, G., Bhat, T. N., Weissig, H., Shindyalov, I. N. and
754 Bourne, P.E.: The protein data bank, *Nucleic. Acids Res.*, 28, 235 – 242, DOI: 10.1093/nar/28.1.235,
755 2000.
- 756 Boisguerin, P., Leben, R., Ay, B., Radziwill, G., Moelling, K., Dong, L. and Volkmer-Engert, R.: An
757 improved method for the synthesis of cellulose membrane-bound peptides with free C termini is
758 useful for PDZ domain binding studies. *Chem. Biol.*, 11, 449 – 459, DOI:
759 10.1016/j.chembiol.2004.03.010, 2004.
- 760 Bui, T. D., Beier, D. R., Jonssen, M., Smith, K., Dorrington, S. M., Kaklamanis, L., Kearney, L.,
761 Regan, R., Sussman, D. J. and Harris, A. L.: cDNA cloning of a human dishevelled DVL-3 gene,
762 mapping to 3q27, and expression in human breast and colon carcinomas. *Biochem. Biophys. Res.*
763 *Commun.*, 239, 510 – 516, DOI: 10.1006/bbrc.1997.7500, 1997.
- 764 Chandanamali, P., Antonio, M. F., Robert, C., Patrick, R. and Naoaki, F.: Sequence and subtype
765 specificity in the high-affinity interaction between human frizzled and dishevelled proteins, *Protein*
766 *Sci.*, 18, 994 – 1002, DOI: 10.1002/pro.109, 2009.
- 767 Chen V. B., Arendall, W. B. 3rd, Headd, J. J. and Keedy, D. A., Immormino, R. M., Karpral, G. J.,
768 Murray, L. W., Richardson, J. S., Richardson, D. C.: MolProbity: all-atom structure validation for
769 macromolecular crystallography. *Acta Cryst.*, 66, 12 - 21, DOI: 10.1107/S0907444909042073, 2010.
- 770 Choi, J., Ma, S.; Kim, H.-Y., Yun, J.-H., Heo, J.-N., Lee, W., Choi, K.-Y. and No, K.: Identification of
771 small-molecule compounds targeting the dishevelled PDZ domain by virtual screening and binding
772 studies. *Bioorg. Med. Chem.*, 24,3259–3266. DOI: 10.1016/j.bmc.2016.03.026, 2016.
- 773 Christensen, N. R., De Luca, M., Lever, M. B., Richner, M., Hansen, A. B., Noes-Holt, G., Jensen, K.
774 L., Rathje, M., Jensen, D. B., Erlendsson, S., Bartling, C. R., Ammendrup-Johnsen, I., Pedersen, S.
775 E., Schönauer, M., Nissen, K. B., Midtgaard, S. R., Teilum, K., Arleth, L., Sørensen, A. T., Bach, A.,
776 Strømgaard, K., Meehan, C. F., Vaegter, C. B., Gether, U. and Madsen, K. L.: A high-affinity,
777 bivalent PDZ domain inhibitor complexes PICK1 to alleviate neuropathic pain. *EMBO Mol. Med.*,
778 12 :e11248, Doi: 10.15252/emmm.201911248, 2020.
- 779 Chuprina, A., Lukin, O., Demoiseaux, R., Buzko, A. and Shivanyuk, A.: Drug- and lead-likeness,
780 target class, and molecular diversity analysis of 7.9 million commercially available organic
781 compounds provided by 29 suppliers. *J. Chem. Inf. Model.*, 50, 470 - 499. Doi: 10.1021/ci900464s,
782 2010.
- 783 Doyle, D. A., Lee, A., Lewis, J., Kim, E., Sheng, M. and MacKinnon, R.: Crystal structures of a
784 complexed and peptide-free membrane protein-binding domain: Molecular basis of peptide
785 recognition by PDZ. *Cell*, 85, 1067-1076, DOI: 10.1016/s0092-8674(00)81307-0, 1996.



- 786 Emsley, P. and Cowtan, K.: Coot: model-building tools for molecular graphics. *Acta Cryst.*, 60, 2126
787 – 2132, DOI: 10.1107/S0907444904019158, 2004.
- 788 Fan, X., Quyang, N., Teng, H. and Yao, H.: Isolation and characterization of spheroid cells from the
789 HT29 colon cancer cell line. *Int. J. Colorect. Dis.*, 26, 1279 - 1285, DOI: 10.1007/s00384-011-1248-
790 y, 2011.
- 791 Fang, L., Von Kries, J. P. and Birchmeier, W.: Identification of small-molecule antagonists of the
792 TCF/ β -catenin protein complex, in 30 years of Wnt signalling. *EMBO Conference: Egmond aan Zee*,
793 Netherlands. p. 101, 2012.
- 794 Fanning, A. S. and Anderson, J. M.: Protein-protein interactions: PDZ domain networks. *Curr. Biol.*,
795 6, 1385 – 1388, DOI: 10.1016/s0960-9822(96)00737-3, 1996.
- 796 Fritzmann, J., Morkel, M., Besser, D., Budezies, J., Kosel, F., Brembeck, F. H., Stein, U., Fichtner, I.,
797 Schlag, P. M. and Birchmeier, W.: A colorectal cancer expression profile that includes transforming
798 growth factor beta inhibitor BAMBI predicts metastatic potential. *Gastroenterology*, 137, 165 - 175,
799 DOI: 10.1053/j.gastro.2009.03.041, 2009.
- 800 Fujii, N., You, L., Xu, Z., Uematsu, K., Shan, J., He, B., Mikami, I., Edmondson, L.R., Neale, G.,
801 Zheng, J., Guy, R. K. and Jablons, D. M.: An antagonist of dishevelled protein-protein interaction
802 suppresses β -catenin-dependent tumor cell growth. *Cancer Res.*, 67, 573 - 579, DOI: 10.1158/0008-
803 5472.CAN-06-2726, 2007.
- 804 Garrett, D. S., Seok Y. J., Peterkofsky A. and Gronenborn, A. M.: Identification by NMR of the
805 binding surface for the histidine-containing phosphocarrier protein HPr on the N-terminal domain of
806 enzyme I of the *Escherichia coli* phosphotransferase system. *Biochem.*, 36, 4393 – 4398, DOI:
807 10.1021/bi970221q, 1997.
- 808 Goddard, T. D. and Kneller, D. G.: SPARKY 3, University of California, San Francisco, 2003.
- 809 Grandy, D., Shan, J., Zhang, X., Rao, S., Akunuru, S., Li, H., Zhang, Y., Alpatov, I., Zhang, X., Lang,
810 R., Shi, De-Li. and Zheng, J.: Discovery and characterization of a small molecule inhibitor of the
811 PDZ domain of dishevelled. *J. Biol. Chem.*, 284, 16256–16263. DOI: 10.1074/jbc.M109.00 9647,
812 2009.
- 813 Hajduk, P. J., Sheppard, G., Nettesheim, D. G., Olejniczak, E. T., Shuker, S. B., Meadows, R. P.,
814 Steinman, D. H., Carrera, G. M. Jr., Marcotte, P. A., Severin, J., Walter, K., Smith, H., Gubbins, E.,
815 Simmer, R., Holzman, T. F., Morgan, D. W., Davidsen, S. K., Summers, J. B. and Fesik, S. W.:
816 Discovery of Potent Nonpeptide Inhibitors of Stromelysin Using SAR by NMR. *J. Am. Chem. Soc.*,
817 119, 5818 – 5827, DOI: 10.1021/ja9702778, 1997.
- 818 Harris, B. Z., Lau, F. W., Fujii, N., Guy, R. K. and Lim, W. A.: Role of electrostatic interactions in
819 PDZ domain ligand recognition. *Biochem.*, 42, 2797-2805, DOI: 10.1021/bi027061p, 2003.
- 820 Hillier, B. J., Christopherson, K. S., Prehoda, K. E., Brecht, D. S. and Lim, W. A.: Unexpected modes
821 of PDZ domain scaffolding revealed by structure of nNOS–syntrophin complex. *Science*, 284, 812–
822 815, 1999.
- 823 Holland, J. D., Klaus, A., Garratt, A. N. and Birchmeier, W.: Wnt signaling in stem and cancer stem
824 cells. *Curr. Opin. Cell Biol.*, 25, 254-264, DOI: 10.1016/j.ceb.2013.01.004, 2013.
- 825 Hori, K., Ajioky, K., Goda, N., Shindo, A., Tagagishi, M., Tenno, T. and Hiroaki, H.: Discovery of
826 Potent Dishevelled/Dvl Inhibitors Using Virtual Screening Optimized With NMR-Based Docking
827 Performance Index. *Front. Pharmacol.*, 9, 983, DOI: 10.3389/fphar.2018.00983, 2018.
- 828 Jain, A.K. and Dubes, R.C. Upper Saddle River, NJ: Prentice Hall, Algorithms for clustering data.
829 320p, 1988.
- 830 Jho, E. H., Zhang, T., Domon, C., Joo, C.-K., Freund, J.-N. and Costantini, F.: Wnt/ β -catenin/Tcf
831 signaling induces the transcription of Axin2, a negative regulator of the signaling pathway. *Mol.*
832 *Cell. Biol.*, 22, 1172 - 1183, DOI: 10.1128/mcb.22.4.1172-1183.2002, 2002.
- 833 Kanwar, S. S., Yu, Y., Nautyal, J., Patel, B. B. and Majumdar, A. P. N.: The Wnt/ β -catenin
834 pathway regulates growth and maintenance of colonospheres. *Mol. Cancer.*, 9, 212, DOI:
835 10.1186/1476-4598-9-212, 2010.
- 836 Kim, H. Y., Choi, S., Yoon, J. H., Lim, H. J., Lee, H., Choi, J., Ro, E. J., Heo, J. N., Lee, W., No, K.
837 T. and Choi, K. Y.: Small molecule inhibitors of the Dishevelled-CXXC5 interaction are new drug
838 candidates for bone anabolic osteoporosis therapy. *EMBO Mol. Med.*, 8, 375-387, DOI:
839 10.15252/emmm.201505714, 2016.
- 840 Klaus, A. and Birchmeier, W.: Wnt signalling and its impact on development and cancer. *Nat. Rev.*
841 *Cancer*, 8, 387-398, DOI: 10.1038/nrc2389, 2008.



- 842 Kurakin, A., Swistowski, A., Wu, S. C. and Bredesen, D. E.: The PDZ domain as a complex adaptive
843 system. *PLoS One*, 2(9), e953, DOI: 10.1371/journal.pone.0000953, 2007.
- 844 Lee, H. J., Wang, N. X., Shi, D. L. and Zheng, J. J.: Sulindac inhibits canonical Wnt signaling by
845 blocking the PDZ domain of the protein dishevelled. *Angew. Chem. Int. Ed. Engl.*, 48, 6448 - 6452,
846 DOI: 10.1002/anie.200902981, 2009.
- 847 Lee, H. J., Wang, X. N., Shao, Y. and Zhenz, J. J.: Identification of tripeptides recognized by the PDZ
848 domain of Dishevelled. *Bioorg. Med. Chem.*, 17, 1701 - 1708, 2009.
- 849 Lewis, A., Segditsas, S., Deheragoda, M., Pollard, P., Jeffery, R., Nye, E., Lockstone, H., Davis, H.,
850 Clark, S., Stamp, G., Poulson, R., Wright, N. and Tomlinson, I.: Severe polyposis in *Apc*(1322T)
851 mice is associated with submaximal Wnt signalling and increased expression of the stem cell marker
852 *Lgr5*. *Gut*, 59, 1680 - 1686, DOI: 10.1136/gut.2009.193680, 2010.
- 853 Lipinski, C. A.: Drug-like properties and the causes of poor solubility and poor permeability. *J.*
854 *Pharmacol. Toxicol. Meth.*, 44, 235 - 249. DOI: 10.1016/S1056-8719(00)00107-6, 2000.
- 855 Lipinski, C. A., Lombardo, F., Dominy, B. W. and Feeney, P. J.: Experimental and computational
856 approaches to estimate solubility and permeability in drug discovery and development settings. *Adv.*
857 *Drug Deliv. Rev.*, 23, 3 - 25. DOI: 10.1016/S0169-409X(96)00423-1, 1997.
- 858 Lv, P. C., Zhu, H. L., Li, H. Q., Sun, J. and Zho, Y.: Synthesis and biological evaluation of pyrazole
859 derivatives containing thiourea skeleton as anticancer. *Bioorg. Med. Chem.*, 18, 4606 - 4614, DOI:
860 10.1016/j.bmc.2010.05.034, 2010.
- 861 Lee, I., Choi, S., Yun, J. H., Seo, S. H., Choi, S., Choi, K. Y. and Lee, W.: Crystal structure of the
862 PDZ domain of mouse Dishevelled 1 and its interaction with CXXC5. *Biochem. Biophys. Res.*
863 *Commun.*, 485, 584-590, DOI: 10.1016/j.bbrc.2016.12.023, 2017.
- 864 Malanchi, I., Peinado, H., Kassen, D., Hussenet, T., Metzger, D., Chambon, P., Huber, M., Hohl, D.,
865 Cano, A., Birchmeier, W. and Huelsken, J.: Cutaneous cancer stem cell maintenance is dependent on
866 beta-catenin signalling. *Nature*, 452, 650 - 653, DOI: 10.1038/nature06835, 2008.
- 867 Mathvink, R. J., Barritta, A. M., Candelore, M. R., Cascieri, M. A., Deng, L., Tota, L., Strader, C. D.,
868 Wyvratt, M. J., Fosher, M. H. and Weber, A. E.: Potent, elective human beta3 adrenergic receptor
869 agonists containing a substituted indoline-5-sulfonamide pharmacophore. *Bioorg. Med. Chem. Lett.*,
870 9, 1869 - 1874, DOI: 10.1016/S0960-894X(99)00277-2, 1999.
- 871 McCoy, A. J., Grosse-Kunstleve, R. W., Adams, P. D., Winn, M. D., Storoni, L. C. and Read, R. J.:
872 Phaser crystallographic software. *J. Appl. Cryst.*, 40(Pt4), 658 - 674, DOI:
873 10.1107/S0021889807021206, 2007.
- 874 McMartin, C. and Bohacek, R. S.: Powerful, rapid computer algorithms for structure-based drug
875 design. *J. Computer-Aided Mol. Des.*, 11, 333 - 344, DOI: 10.1023/a:1007907728892, 1997.
- 876 Mizutani, K., Miyamoto, S., Nagahata, T., Konishi, N., Emi, M. and Onda, M.: Upregulation and
877 overexpression of DVL1, the human counterpart of the *Drosophila* Dishevelled gene, in prostate
878 cancer. *Tumori*, 91, 546 - 551, 2005.
- 879 Molenaar, M., van de Wetering, M., Oosterwegel, M., Peterson-Maduro, J., Godsave, S., Korinek,
880 V., Roose, J., Destree, O. and Clevers, H.: XTcf-3 transcription factor mediates beta-catenin-induced
881 axis formation in *Xenopus* embryos. *Cell*, 86, 391 - 399, DOI: 10.1016/S0092-8674(00)80112-9,
882 1996.
- 883 Mosmann, T.: Rapid colorimetric assay for cellular growth and survival: application to proliferation
884 and cytotoxicity assays. *J. Immunol. Methods*, 65, 55 - 63, DOI: 10.1016/0022-1759(83)90303-4,
885 1983.
- 886 Murshudov, G. N., Vagin, A. A. and Dodson, E. J.: Refinement of macromolecular structures by the
887 maximum-likelihood method. *Acta Cryst.*, 53, 240 - 255, DOI: 10.1107/S0907444996012255, 1997.
- 888 O'Brien, P. M., Ortwine, D. F., Pavlovsky, A. G., Picard, J. A., Sliskovic, D. R., Roth, B. D., Dyer, R.
889 D., Johnson, L. L., Man, C. F. and Hallak, H.: Structure-activity relationships and pharmacokinetic
890 analysis for a series of potent, systemically available biphenylsulfonamide matrix metalloproteinase
891 inhibitors. *J. Med. Chem.*, 43, 156 - 166, DOI: 10.1021/jm9903141, 2000.
- 892 Osada, R., Funkhouser, T., Chazelle, D. and Dobkin, D.: Shape distributions, *ACM Transactions on*
893 *Graphics*, 21(4), 807 - 832, DOI: 10.1145/571647.571648, 2002
- 894 Pawson, T.: Dynamic control of signalling by modulator adaptor proteins. *Curr. Opin. Cell Biol.*, 19,
895 112 -116, DOI: 10.1016/j.ceb.2007.02.013, 2007.
- 896 Polakis, P.: Drugging Wnt signaling in cancer. *EMBO J.*, 31, 2737-2746, DOI:
897 10.1038/emboj.2012.126, 2012.



- 898 Ponting, C. P., Phillips, C., Davies, K. E. and Blake, D. J.: PDZ domains: targeting signalling
899 molecules to submembranous sites. *Bioassays*, 19, 469 – 479, DOI: 10.1002/bies.950190606, 1997.
- 900 Puranik, P., Aakanksha, K., Tadas, S. V., Robert, D. B., Lalji, K. G. and Vincent, C. O. N.: Potent
901 anti-prostate cancer agents derived from a novel androgen receptor down-regulating agent. *Bioorg.*
902 *Med. Chem.*, 16, 3519 – 3529, DOI: 10.1016/j.bmc.2008.02.031, 2008.
- 903 Riese, J., Yu, X., Munnerly, A., Eresh, L., Hsu, S.-C., Grosschedl, R. and Bienz, M.: LEF-1, a nuclear
904 factor coordinating signaling inputs from wingless and decapentaplegic. *Cell*, 88, 777 – 787, DOI:
905 10.1016/s0092-8674(00)81924-8, 1997.
- 906 Rimbault, C., Maruthi, K., Breillat, C., Genuer, C., Crespillo, S., Puente-Muñoz, V., Chamma, I.,
907 Gauthereau, I., Antoine, S., Thibaut, C., Tai, F. W. J., Dartigues, B., Grillo-Bosch, D., Claverol, S.,
908 Poujol, C., Choquet, D., Mackereth, C. D. and Sainlos, M.: Engineering selective competitors for the
909 discrimination of highly conserved protein-protein interaction modules. *Nat. Commun.*, 10, 4521,
910 DOI: 10.1038/s41467-019-12528-4, 2019.
- 911 Sack, U., Walther, W., Scudiero, D., Selby, M., Aumann, J., Lemos, C., Fichtner, I., Schlag, P. M.,
912 Shoemaker, R. H. and Stein, U.: S100A4-induced cell motility and metastasis is restricted by the
913 Wnt/beta-catenin pathway inhibitor calcimycin in colon cancer cells. *Mol. Biol. Cell.*, 22, 3344 -
914 3354, DOI: 10.1091/mbc.E10-09-0739, 2011.
- 915 Sanner, M. F., Olson, A. J. and Spohner, J. C.: Reduced surface: an efficient way to compute molecular
916 surfaces, *Biopolymers*, 38, 305 – 320, DOI: 10.1002/(SICI)1097-0282(199603)38:3%3C305::AID-
917 BIP4%3E3.0.CO;2-Y, 1996.
- 918 Saupe, J., Roske, Y., Schillinger, C., Kamdem, N., Radetzki, S., Diehl, A., Oschkinat, H., Krause, G.,
919 Heinemann, U. and Rademann, J.: Discovery, structure-activity relationship studies, and crystal
920 structure of non-peptide inhibitors bound to the Shank3 PDZ domain. *ChemMedChem*, 6, 1411 -
921 1422, DOI: 10.1002/cmdc.201100094, 2011.
- 922 Schultz, J., Hoffmüller, U., Krause, G., Ashurts, J., Macias, M. J., Schmieder, P., Schneider-Mergener,
923 J. and Oschkinat, H.: Specific interactions between the syntrophin PDZ domain and voltage-gated
924 sodium channels. *Nat. Struct. Biol.*, 5, 19 – 24, DOI: 10.1038/nsb0198-19, 1998.
- 925 Shan, J., Shi, D. L., Wang, J. and Zheng, J.: Identification of a specific inhibitor of the dishevelled
926 PDZ domain. *Biochem.*, 44, 15495-15503, DOI: 10.1021/bi0512602, 2005.
- 927 Shan, J., Zhang, X., Bao, J., Cassell, R. and Zheng, J. J.: Synthesis of potent Dishevelled PDZ domain
928 inhibitors guided by virtual screening and NMR studies, *Chem. Biol. Drug. Des.*, 79, 376 – 383,
929 DOI: 10.1111/j.1747-0285.2011.01295.x, 2012.
- 930 Sheng, M. and Sala, C.: PDZ domains and the organization of supramolecular complexes. *Annu. Rev.*
931 *Neurosci.*, 24, 1 – 29, DOI: 10.1146/annurev.neuro.24.1.1, 2001.
- 932 Sievers, F., Wilm, A., Dineen, D. G., Gibson, T. J., Karplus, K., Li, W., Lopez, R., McWilliam, H.,
933 Remmert, M., Söding, J., Thompson, J. D. and Higgins, D. G.: Fast, Scalable generation of high-
934 quality protein multiple sequence alignments using Clustal Omega. *Mol. Syst. Biol.*, 7, 539,
935 Doi:10.1038/msb.2011.75, 2011.
- 936 Sineva, G. S. and Pospelov, V. A.: Inhibition of GSK3beta enhances both adhesive and signalling
937 activities of beta-catenin in mouse embryonic stem cells. *Biol. Cell*, 102, 549-560, DOI:
938 10.1042/BC20100016, 2010.
- 939 Sleight, A. J., Boess, F. G., Bös, M., Levet-Trafit, B., Riemer, C. and Bourson, A. Br.:
940 Characterization of Ro 04-6790 and Ro 63-0563: potent and selective antagonists at human and rat
941 5-HT6 receptors. *J. Pharmacol.*, 124, 556 - 562, DOI: 10.1038/sj.bjp.0701851, 1998.
- 942 Songyang, Z., Fanning, A. S., Fu, C., Xu, J., Marfatia, S. M., Chisti, A. H., Crompton, A., Chan, A.
943 C., Anderson, J. M. and Cantley, L. C.: Recognition of unique carboxyl-terminals motifs by distinct
944 PDZ domains. *Science*, 275, 73 - 77, DOI: 10.1126/science.275.5296.73, 1997.
- 945 Shuker, S. B., Hajduk, P. J., Meadows, R. P. and Fesik, S. W.: Discovering high-affinity ligands for
946 proteins: SAR by NMR. *Science*, 274, 1531 – 1534, DOI: 10.1126/science.274.5292.1531, 1996.
- 947 Shuker, S. B., Hajduk, P. J., Meadows, R. P. and Fesik, S. W.: Discovering high-affinity ligands for
948 proteins: SAR by NMR. *Science*, 274, 1531 – 1534, DOI: 10.1126/science.274.5292.1531, 1996.
- 949 Tellew, J. E., Baska, R. A. F., Beyer, S. M., Carlson, K. E., Cornelius, L. A., Fadnis, L., Gu, Z., Kunst,
950 B. L., Kowala, M. C., Monshizadegan, H., Murugesan, N., Ryan, C. S., Valentine, M. T., Yang, Y.
951 and Macor, J. E.: Discovery of 4-[(imidazol-1-yl)methyl]biphenyl-2-sulfonamides as dual
952 endothelin/angiotensin II receptor antagonists. *Bioorg. Med. Chem. Letters*, 13, 1093 – 1096, DOI:
953 10.1016/s0960-894x(03)00018-0, 2003.



- 954 [The PyMOL Molecular Graphics System, Version 2.3.4 Schrödinger, LLC](#)
955 Uematsu, K., He, B., You, L., Xu, Z., McCormick, F. and Jablons, D. M.: Activation of the Wnt
956 pathway in non-small cell lung cancer: evidence of dishevelled overexpression. *Oncogene*, 22, 7218
957 - 7221, DOI: 10.1038/sj.onc.1206817, 2003.
958 Uematsu, K., Kanazawa, S., You, L., He, B., Xu, Z., Li, K., Peterlin, B. M., McCormick, F. and
959 Jablons, D. M.: Wnt pathway activation in mesothelioma: evidence of dishevelled overexpression and
960 transcriptional activity of β -catenin. *Cancer Res.*, 63, 4547 – 4551, 2003.
961 Vermeulen, L., De Sousa E Melo, F., van der Heijden, M., Cameron, K., de Jong, J. H., Borovski, T.,
962 Tuynman, J. B., Todaro, M., Merz, C., Rodermond, H., Sprick, M. R., Kemper, K., Richel, J. J.,
963 Stassi, G. and Medema, J. P.: Wnt activity defines colon cancer stem cells and is regulated by the
964 microenvironment. *Nat. Cell. Biol.*, 12, 468 - 476, DOI: 10.1038/ncb2048, 2010.
965 Wallingford, B. J. and Raymond H.: The developmental biology of Dishevelled: an enigmatic protein
966 governing cell fate and cell polarity. *Development*, 132, 4421 - 4436, DOI: 10.1242/dev.02068,
967 2005.
968 Wang, C., Dai, J., Sun, Z., Shi, C., Cao, H., Chen, X., Gu, S., Li, Z., Qian, W. and Han, X.: Targeted
969 inhibition of dishevelled PDZ domain via NSC668036 depresses fibrotic process. *Exp. Cell Res.*,
970 331, 115 – 122, DOI: 10.1016/j.yexcr.2014.10.023, 2015.
971 Weeraratna, A. T., Jiang, Y., Hostetter, G., Rosenblatt, K., Duray, P., Bittner, M. and Trent, J. M.:
972 Wnt5a signalling directly affects cell motility and invasion of metastatic melanoma. *Cancer Cell*, 1,
973 279 – 288, DOI: 10.1016/s1535-6108(02)00045-4, 2002.
974 Wong, H. C., Bourdelas, A., Krauss, A., Lee, H. J., Shao, Y., Wu, D., Mlodzik, M., Shi, D. L. and
975 Zheng, J.: Direct binding of the PDZ domain of Dishevelled to a conserved internal sequence in the
976 C-terminal region of Frizzled. *J. Mol. Cell*, 12, 1251 -1260, DOI: 10.1016/s1097-2765(03)00427-1,
977 2003.
978 Wong, H., Mao, J., Nguyen, J. T., Srinivas, S., Zhang, W., Liu, B., Li, L., Wu, D. and Zheng, J.:
979 Structural basis of the recognition of the dishevelled DEP domain in the Wnt signalling pathway.
980 *Nat. Struct. Biol.*, 7, 1178 -1184, DOI: 10.1038/82047, 2000.
981 Wu, C., Decker, E. R., Blok, N., Bui, H., Chen, Q., Raju, B., Bourgoyne, A. R., Knowles, V.,
982 Biediger, R. J., Market, R. V., Lin, S., Dupre, B., Kogan, T. P., Holland, G. W., Brock, T. A. and
983 Dixon, R. A. F.: Endothelin antagonists: substituted mesitylcarboxamides with high potency and
984 selectivity for ET(A) receptors. *J. Med. Chem.*, 42, 4485 - 4499, DOI: 10.1021/jm9900063, 1999.
985 Zartler, E. R. and Shapiro, M. J.: Protein NMR-based screening in drug discovery. *Curr. Pharm. Des.*,
986 12, 3963 – 3972, DOI: 10.2174/138161206778743619, 2006.
987 Zartler, E. R., Hanson, J., Jones, B. E., Kline, A. D., Martin, G., Mo, H., Shapiro, M. J., Wang, R.,
988 Wu, H. and Yan, J.: RAMPED-UP NMR: multiplexed NMR-based screening for drug discovery. *J.*
989 *Am. Chem. Soc.*, 125, 10941 - 10946, DOI: 10.1021/ja0348593, 2003.
990 Zhang, M. and Wang, W.: Organization of signalling complexes by PDZ-domain scaffold proteins.
991 *Acc. Chem. Res.*, 36, 530 – 538, DOI: 10.1021/ar020210b, 2003.
992 Zhang, M. and Wang, W.: Organization of signalling complexes by PDZ-domain scaffold proteins.
993 *Acc. Chem. Res.*, 36, 530 – 538, DOI: 10.1021/ar020210b, 2003.
994 Zhang, Y., Appleton, B. A., Wiesmann, C., Lau, T., Costa, M., Hannoush, R. N. and Sidhu, S. S.:
995 Inhibition of Wnt signaling by Dishevelled PDZ peptides. *Nat. Chem. Biol.*, 5, 217 -219, DOI:
996 10.1038/nchembio.152, 2009.